A UNIAXIAL STRESS ANALYSIS OF THE BERYLLIUM PAIR BOUND EXCITON ABSORPTION SPECTRUM IN SILICON

Thesis for the Degree of M.Sc.

Presented to

THE NATIONAL COUNCIL FOR EDUCATIONAL AWARDS

by

Keith A. Moloney

SCHOOL OF PHYSICAL SCIENCES

THE NATIONAL INSTITUTE FOR HIGHER EDUCATION

DUBLIN

Research Supervisor: Dr. Martin O. Henry

Abstract

The low temperature luminescence spectrum of silicon doped with beryllium has been found to contain a strong set of no-phonon lines centred around 1.077 eV with phonon assisted replicas at lower energies. The energies of these transitions are as would be expected for an isoelectronic bound exciton (IBE). The thermalization of the no-phonon lines follows the pattern of an exciton bound to an axially symmetric centre.It has already been proposed that when Be is doped into Si the majority of the Be forms substitutional-interstitial pairs, which would be axial isoelectronic centres. The strength and lifetimes of the absorption lines of the centre are consistent with the IBE assignment. Zeeman studies of the luminescence spectra show that the centre has a <100> axis.

The temperature variations in the phonon sidebands are not obviously distinctive of either a donor or an acceptor-like IBE. However while the series of excited states of the exciton as observed in absorption cannot be fitted to a donor series it is found to match exactly that of the boron acceptor in silicon. In this study the absorption spectrum of the centre is examined under uniaxial stress to try to determine conclusively the nature, whether donor or acceptor-like, of the centre.

The absorption lines of interest coincide with a region of strong water vapour absorption and under stress many of the lines are extremely weak. To obtain usable data the spectra are normalised with respect to a previously recorded standard containing only the water vapour absorption. This process is performed by a microcomputer and not only greatly enhances the features of interest but also removes the need to calibrate the system as any variations with wavelength in the output of the light source, the response of the spectrometer and the sensitivity of the detector are compensated for automatically. Several aspects of the results obtained are examined and all are found to be consistent with the acceptor-like classification.

The work recorded in this thesis has been reported in the following paper published in the Journal of Physics:

Uniaxial stress studies of the Be pair bound exciton absorption spectrum in silicon.

M O Henry, Keith A Moloney, J Treacy, F J Mulligan and E C Lightowlers.

J. Phys. C : Solid State Physics 17 (1984) 6245-51

CONTENTS

	Page
Chapter 1 : Introduction	
1.1 Introduction	1
1.2 Donors and Acceptors	5
1.3 Symmetry	8
1.4 Excitons	11
1.5 Silicon exciton spectra	14
Chapter 2 : The Beryllium pair centre in Silicon	
2.1 Introduction	17
2.2 Luminescence spectra	18
2.3 Classification of the centre	22
2.4 Conclusion	25
Chapter 3 : Experimental Methods	
3.1 Introduction	26
3.2 General	27
3.3 Stress rig and sample holder	35
3.4 Signal processing	37
Chapter 4 : Results	
4.1 Introduction	44
4.2 Results	45

Chapter 5 : Analysis

5.1 Introduction 54

5.2 Uniaxial stress analysis 55

5.3 Stress induced splitting patterns 59

5.4 Deformation potentials 63

5.5 Dissociation of the exciton 65

5.6 Conclusion 67

Chapter 6 : Conclusion 68

Appendix 1

P.C.B. layout of spike removal unit 69

Appendix 2

Program to control monochromator and to record and process spectra 71

Appendix 3

Estimation of deformation potentials 75

References 77

Acknowledgements 79

CHAPTER 1

INTRODUCTION

1.1 Introduction

An ideal silicon crystal, completely pure with all the atoms stationary at their lattice sites, would be a perfect periodic array and its electronic states would therefore be those of electrons in a periodic potential. Bloch theory describes completely this idealised situation and states that the eigenstates of electrons in such a potential can be chosen to be of the form:

$$\psi_{nk}(r) = U_{nk}(r)e^{ik\cdot r} \qquad (1.1)$$

where U_{nk} has the periodicity of the lattice and k, the wave vector, is a reciprocal lattice vector confined within the Brillouin zone. The index n indicates that for each value of k there are many different possible wavefunctions. For each n there are an infinite number of discrete energy eigenstates, each corresponding to a different k, called an energy band. The band structure of a crystal is the variation of energy with k for the different bands. A plot of part of the band structure of silicon is given in figure 1.1. To determine the ground state of a crystal the electrons are taken to occupy the lowest energy states available. Two possible

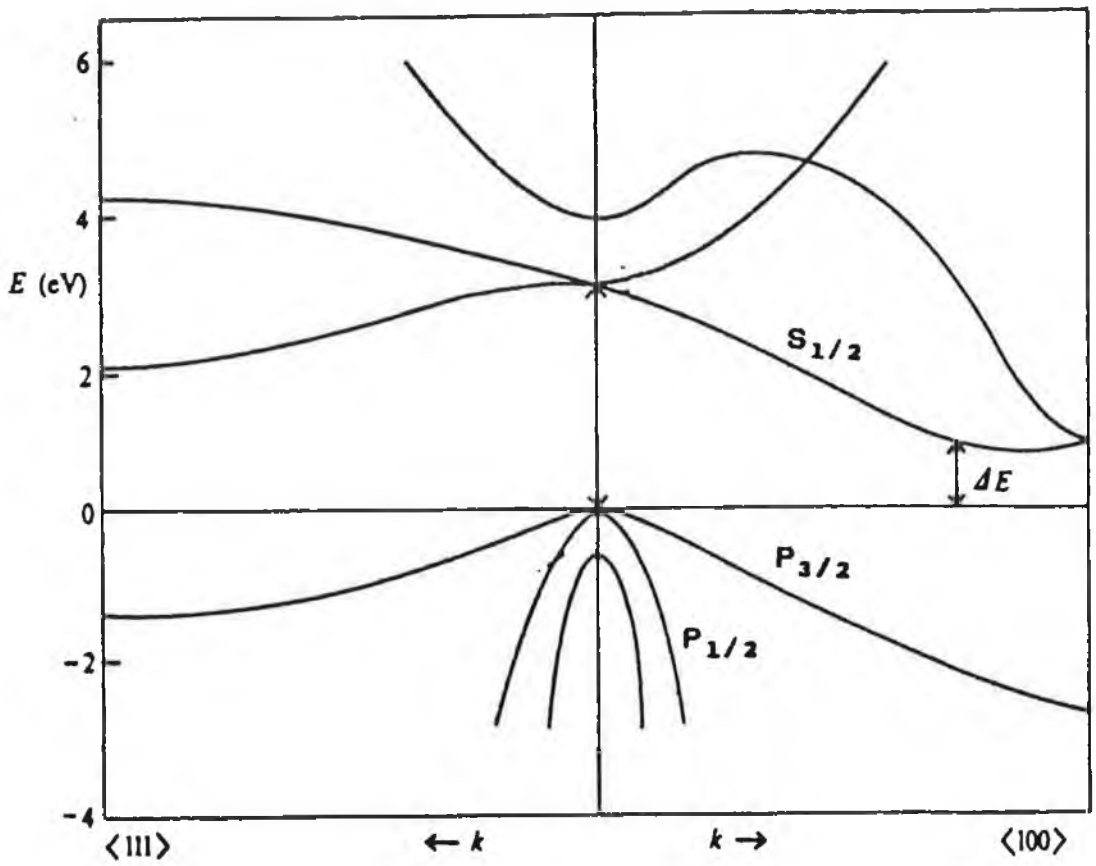

Fig 1.1 : Part of the electronic band structure of silicon.
Silicon is an indirect gap semiconductor with six equivalent conduction band minima located about 80% of the way to the zone boundry along the ‹100› directions. The valence band maximum occurs at k=0 where two degenerate bands with different curvatures meet giving rise to holes with different effective masses. The $P_{3/2}$ band maximum is fourfold degenerate while the $P_{1/2}$ maximum is doubly degenerate.

configurations result: one in which several bands are partially filled, the highest occupied level lying within a band. This is the case in metals. In the other some bands are completely filled and all others are empty with an energy gap between the filled and empty bands. If the energy gap is small (<2 eV) a semiconductor results; otherwise the crystal is an insulator. The band gap of silicon is 1.12 eV (at 300 K). A semiconductor is classified as either direct or indirect gap depending on whether the lowest energy in the conduction band and the highest energy in the valence band occur at the same value of k or not. As is clear from figure 1.1 silicon is an indirect gap semiconductor. If an electron is excited from the valence band to the conduction band it leaves a vacant state behind called a hole which behaves as a positive particle similar to an electron. Both the electron and the hole are free to move through the crystal. From the motion of electrons and holes in applied electric fields it is found that they behave as if their mass was lower than the actual electron mass. The value of this effective mass depends on the k value of the state occupied by the electron. The product $\hbar k$ is called the crystal momentum and its rate of change is equal to the applied external force. It is analogous to the linear momentum of a free electron and is a conserved quantity.

A crystal can absorb a photon and excite an electron from an initial state of energy E_i to a final state of higher

energy E_f. The selection rules governing such transitions , from the conservation of energy and crystal momentum are

$$E_f - E_i = hf \qquad (1.2)$$

$$k_f - k_i = 0 \qquad (1.3)$$

where f is the frequency of the light, k_i and k_f are the wavevectors of the initial and final states respectively; the wavevector of the photon is negligible in comparison. Thus in a perfect crystal only direct transitions, between states with the same wavevector, and of an energy greater than the band gap, occur in absorption.

In reality however the atoms of the crystal will vibrate at all temperatures causing a deviation from perfect periodicity. The vibrations of a lattice are characterised by a frequency ω and wavevector k_p. The relationship between these is not linear. The vibrations are quantized into units called phonons each of energy $\hbar\omega$ and crystal momentum $\hbar k$. An indirect transition is possible if a phonon is also involved in the electron-photon interaction. The selection rules now become

$$E_f - E_i = hf \pm \hbar\omega \qquad (1.4)$$

$$k_f - k_i = k_p \qquad (1.5)$$

This means that in absorption if a phonon already present in the lattice is involved transitions can occur for energies less than the band gap. These indirect transitions have a lower probability than direct transitions. Another possibility results from the fact that all crystals contain impurities which destroy the periodicity of the lattice; as a result a transition can occur in the vicinity of a defect in which crystal momentum is not conserved, i.e. indirect transitions may take place without phonons.

1.2 Donors and Acceptors

Impurities in a semiconductor crystal change its properties markedly; by providing new carriers they increase the conductivity and by introducing new energy levels they change absorption and emission spectra. Under suitable conditions they can bind electrons or holes. Chemical impurities are divided into three classes: neutral, donor and acceptor. Neutral impurity centres are ones which produce no change in conductivity and include isoelectronic centres which have the same number of valence electrons as the host. An impurity which increases the conductivity by supplying extra conduction electrons is called a donor. Consider a group V element such as phosphorous substituting for a silicon atom. Four of its five electrons will form covalent bonds with the four nearest silicon atoms. The fifth electron cannot bond

and is available to the conduction band. However, the P atom left behind is now a positive ion and the electron will be bound to it. The binding energy will be much less than the first ionization potential of P because the electron is not in free space but in the crystal. This is due to two factors. Firstly the electric field of the ion is reduced by the static dielectric constant(ϵ) of silicon. Secondly, in the crystal, electrons move under external fields as particles with an effective mass m^*. The problem is similar to a hydrogen atom if the electron mass is replaced by m^* and the charge by e/ϵ. Thus a series of bound states exists of radius r_n and binding energy E_n given by

$$r_n = \frac{n^2h^2\epsilon}{\Pi m^* e^4} \qquad (1.6)$$

$$E_n = \frac{m^* e^4}{8h^2\epsilon^2 n^2} \qquad (1.7)$$

As the electron is in the crystal where the equivalent of a free electron is one in the conduction band the binding energy is with respect to the bottom of the conduction band. Also shallow impurity states must be formed from crystal states so the electron is taken to be in a state at the bottom of the conduction band perturbed by the potential of the donor ion. There are six equivalent minima in the conduction band of silicon and Kohn and Luttinger (1955) have shown that a donor

state is a combination of these six states multiplied by a hydrogenic envelope function. The envelope functions are split by the crystal field so that there are more non degenerate levels than for hydrogen, e.g. the 1s ground state is split into three orbitally non-degenerate states. The effective mass theory outlined above predicts the same binding energy for all donors in silicon. This is not correct,as although the spacing of excited states of different donors are more or less the same, their ground state energies are not. This is because an electron in the ground state is localised at the impurity site and therefore more sensitive to the exact nature of the dopant.

An acceptor is an impurity which increases the conductivity by providing extra holes in the valence band. When a group III element is substituted for a silicon atom it can form only three covalent bonds so that there is a vacant electron state, or a hole, bound to the impurity. It too has a hydrogenic series of energy levels near the valence band edge. In this case the states are formed from the states at the top of the valence band. The hydrogenic series of levels predicted by effective mass theory correspond to optical spectra which lie in the infra-red . These spectra have been studied at low temperature using a variety of techniques. A review of the theory and experimental results of the spectroscopy of donor and acceptor states in semiconductors has been given by Ramdas and Rodrigues (1981).

1.3 Symmetry

If a system is symmetric with respect to a transformation of co-ordinates then that transformation leaves the system unchanged. Therefore the transformed Hamiltonian (H') is identical to the original Hamiltonian (H). Thus if one transforms the Schrodringer equation one gets

$$H'\Psi' = E\Psi' \Rightarrow H\Psi' = E\Psi' \quad \text{as } H' = H \qquad (1.8)$$

Thus any symmetry leads to degeneracy; the greater the degree of symmetry the higher the multiplicity of the degeneracy.

A single atom in free space has full rotational symmetry but an atom in a crystal does not; its symmetry is determined by that of the lattice. Thus its energy levels will be less degenerate than those of a free atom. From a detailed study of the symmetry properties of the crystal one can determine the number of possible energy levels and their degeneracy.

The symmetry elements of a crystal form a group and therefore are handled using group theory in which a group is represented by a set of matrices which satisfy the same multiplication table as the group. These matrices give the projections of the states onto the basis vectors of a linear vector space which is invariant under the operation of the

group elements. There are an infinite number of such representations but only a small number of ones which cannot be made up from simpler representations and are not related to each other by similarity transforms; these are called inequivalent irreducible representations. Groups are divided into sets of conjugate elements called classes. For example, all rotations through the same angle form a class. Because they are conjugate, all the matrices representing members of a class have the same trace. This is called the character of the class. It can be shown that the number of inequivalent irreducible representations is equal to a number of classes and that the square of the dimension of the representations equals the number of elements in the group. Therefore merely from the number of group elements and classes one can get the number of irreducible representations. A group is described by a character table which gives the character of each class for each of the irreducible representations.

All wavefunctions of the Hamiltonian corresponding to the same energy level form a vector space. This vector space is invariant under the transformations of the symmetry group (T_g) of the Hamiltonian as

$$H\Psi' = HT_g\Psi = T_gH\Psi = T_gE\Psi = E\Psi' \qquad (1.9)$$

Because of this, transforming one eigenfunction yields another. Thus one can form an irreducible representation

using the eigenfunctions as basis vectors. From the symmetry of the system one knows the group of the Hamiltonian and therefore the number and dimensionality of its irreducible representations. Thus each energy level of the system must correspond to one of the representations and simply by knowing the group and its character table one can determine the degeneracy of the possible energy levels. If the system is perturbed so that the symmetry is lowered, for example by stress, then the number of group elements is reduced and the original irreducible representations are now reducible. From the character tables one can determine how these representations will reduce and therefore the number of levels into which corresponding states of the original system will split. Group theory and its application to energy level splitting patterns is described in many texts (eg Tinkham 1964, Heine 1964, Elliott and Dawber 1979). The symmetry properties of impurity states in semiconductors have been reviewed by Fisher and Ramdas (1969). For a single electron or hole in silicon the appropriate group is the double group T_d' . This group has eight different irreducible representations. Γ_1 and Γ_2 are one dimensional, Γ_3, Γ_6 and Γ_7 are two dimensional, Γ_4 and Γ_5 are three dimensional and Γ_8 is four dimensional. The possible classifications for electron states are Γ_1, Γ_2, Γ_3, Γ_4 and Γ_5 while the hole states are, in order of increasing energy, Γ_8, Γ_6 and Γ_7 (Chandrasekaer et al 1973).

1.4 Excitons

The description of interband transitions given above ignores the possibility of interaction between the excited electron in the conduction band which has made the transition and the hole created by its absence in the valence band. Obviously as these two particles are oppositely charged they will be attracted to each other thereby lowering the energy of the final state, making it a state whose energy lies within the band gap. Such an electron hole pair bound together is called an exciton. As mentioned earlier both electrons in the conduction band and holes in the valence band are free to move through the crystal. Consequently an exciton can move, the pair being held together by their mutual attraction. This is called a Wannier free exciton. The binding energy of the free exciton in silicon is 14.7 meV (Shaklee and Nahory 1970). If one of the particles is attracted to a centre in the crystal it can become trapped and the other particle is held by its attraction to the first so that the exciton is localised about the centre. This is one mechanism for the formation of a bound exciton (BE). The binding of the exciton to the trap further lowers the energy of the exciton by an amount equal to the characteristic binding energy of that trap.

Many types of centre can trap an exciton including ionized or neutral donors and acceptors and isoelectronic centres. Not all isoelectronic centres can bind excitons, in particular

substitutional isoelectronic atoms which are very similar to the host, such as C in Si, may not. As isoelectronic centres are neutral the binding force is not electrostatic but some other short range force. The origin and nature of this force are not well understood. Hopfield et al (1966) developed a model for isoelectronic bound excitons (IBE) based on the sequential trapping of the electron-hole pair, first one particle is trapped by the centre then the other is held by its electrostatic attraction to the first. IBE can then be divided into two types, donor-like in which the hole is trapped first and acceptor-like in which the electron is trapped first. It is very difficult to predict which particle of an exciton a centre will attract. The model assumes that the inner particle is tightly held in a non-degenerate s like state and does not undergo excitation to higher states. Because the hole of an acceptor-like IBE sees largely the same field as the hole bound to any acceptor it has a series of bound states with splittings similar to those of an acceptor but of course with a different ground state energy. Similarly a donor-like IBE has a series of levels characteristic of a donor impurity.

There are two possible schemes by which one can describe exciton states. In the first (Kirczenow 1977) the electron and hole are taken to be quasi-independent and each is labelled according to the appropriate irreducible representation, those of the band extrema . The exciton state

is the combination of these written for an electron and a hole, for example, (Γ_1,Γ_8). This ignores the possibility of exchange interaction between the particles. Given the large separation of the particles one can assume that exchange interaction is only significant for the ground state. The second description then is that in which the pair is described as normal for two spin a half particles under exchange coupling . The exciton is described by a total angular momentum quantum number J and its projection in the z direction M_j . These are obtained from the addition of electron and hole quantum numbers which are those of the band extrema . Because the electron and hole are oppositely charged the state with the highest J value has the lowest energy. States with different M_j values but the same J value are degenerate unless some strain introduces a preferred z direction. These two descriptions, in terms of either irreducible representations or angular momentum quantum numbers, are completely compatible ; each irreducible representation corresponds to a state with different angular momentum and one can transform from one to the other by suitable unitary transformations (Kiloran et al 1982). In this work both descriptions are used; the description used in each discussion being the more convenient one.

1.5 Silicon Exciton Spectra

By studying the exciton bound to it one can gain information about a trapping centre. This information is obtained from the absorption and emission spectra of the exciton, the selection rules deduced from these and the way all these vary when the system is perturbed. Although no-phonon lines are forbidden for the free exciton, strong no-phonon lines are observed in both the emission and absorption spectra of BE as crystal momentum need not be conserved in the vicinity of a defect. Radiative recombination is the dominant process for IBE, as there are only two particles present, whereas excitons bound to other types of centre can decay via an Auger process involving another charged particle such as the electron of a donor or the hole of an acceptor. In the three particle process the exciton recombines transferring all the energy to the third particle which is excited high into the appropriate band. The third particle then decays by phonon emission so that the Auger process is completely non-radiative. The transition probability of the Auger is typically upto 500 times that of the radiative recombination so that the spectral lines of IBE are much stronger with longer lifetimes than those of other bound excitons.

Very low temperature photoluminescence reveals details of the ground state of the exciton as it is the only occupied level.

Using the particle exchange description the different transitions observed can be explained in terms of the recombination of excitons with different angular momenta. The exciton wavefunction is formed from electron and hole eigenfunctions $|J,M_j\rangle$. The electron states, coming from $S_{1/2}$ like conduction band, are $|1/2,\pm1/2\rangle$ and the hole states, coming from the $P_{3/2}$ like valence band, are $|3/2,\pm1/2\rangle$ and $|3/2,\pm3/2\rangle$. These combine through coulomb exchange coupling to form exciton states $|J,M_j\rangle$, a triplet J=1 and a quintuplet J=2. The final state is the ground state of the crystal which has J=0. The spectral lines corresponding to transitions from states of J=2 are called B lines while those from J=1 states are A lines. B lines are generally much weaker than A lines as they result from forbidden transitions, the relevant selection rule being $\Delta J = 0,1$. At the lowest temperatures only the very lowest energy states, the J=2 states, will be occupied and only B line emission will be observed. At slightly higher temperatures the J=1 states will be populated and the A line will be observed. In absorption only allowed transitions are observed and the B lines are not seen. However transitions to excited states of the exciton may be detected as well as the A line to the ground state.

Bound exciton states are very common in practical semiconductors as they are deliberately doped, to control electrical properties and to enhance radiative recombination,

with impurities which can trap excitons. These BE states are interesting because they both characterize the impurities which bind them and provide information on the semiconductor itself. As exciton states are best examined spectroscopically BE spectra are a very rewarding topic of study.

CHAPTER 2

The Beryllium Pair Centre in Silicon

2.1 Introduction

Even though excitons bound at isoelectronic centres in II-VI and III-V semiconductors have been extensively studied, (Dean and Herbert (1979) provide a good review) it is only recently, since about 1980, that isoelectronic exciton trapping centres in silicon have been studied in detail. Watkins et al (1984) list the majority of IBE reported in silicon to date. Such centres differ from similar centres in other semi-conductors, such as GaP, in that there are no point isoelectronic defects in silicon and many of the traps in it have only been tentatively identified, if at all. An exception is the beryllium related isoelectronic trap. When this group II element is diffused into high resistivity silicon two acceptor centres are formed, one due to isolated substitutional beryllium atoms, the other due to some unknown beryllium aggregate (Crouch et al (1972)). Mass spectroscopy shows that these two centres account for only 10% of Be atoms present. The remainder must be present in some neutral configuration and as Be has two valence electrons a pair of Be atoms, one substitutional the other interstitial, would form an isoelectronic centre. This centre could be expected to trap excitons.

2.2 Luminescence Spectra

Low temperature photoluminescence of Be doped Si (Henry et al (1981)) confirms this expectation. The spectrum, shown in figure 2.1, consists of a strong sharp set of no-phonon lines at about 1.077 eV with well resolved phonon replicas at lower energies. The wavelength of the emission indicates that it is due to bound exciton recombination and the efficiency suggests that the recombination takes place at an isoelectronic centre. The temperature dependence of the intensities of the no-phonon lines between 2K and 13K, figure 2.2, is similar to that expected for electron-hole recombination at an isoelectronic centre with axial symmetry, such as a Be pair. Morgan and Morgan (1970) have described in detail the states of excitons bound to axially symmetric centres. As mentioned earlier the electron and hole states combine through coulomb exchange coupling to form triplet J=1 and quintuplet J=2 exciton states. However due to the presence of the axial strain in the z direction, states with different M_j values are no longer degenerate. Thus as a result of the exchange interaction and the axial strain five states are produced in order of decreasing energy $|1,0\rangle$, $|1,\pm1\rangle$, $|2,0\rangle$, $|2,\pm1\rangle$, $|2,\pm2\rangle$. The selection rule for transitions between states described by J-J coupling is $\Delta J = 0,\pm1$. The final state of recombined electron and hole is $|0,0\rangle$, thus only transitions from the $|1,0\rangle$ and the $|1,\pm1\rangle$ states are electric dipole allowed. However, the axial strain not

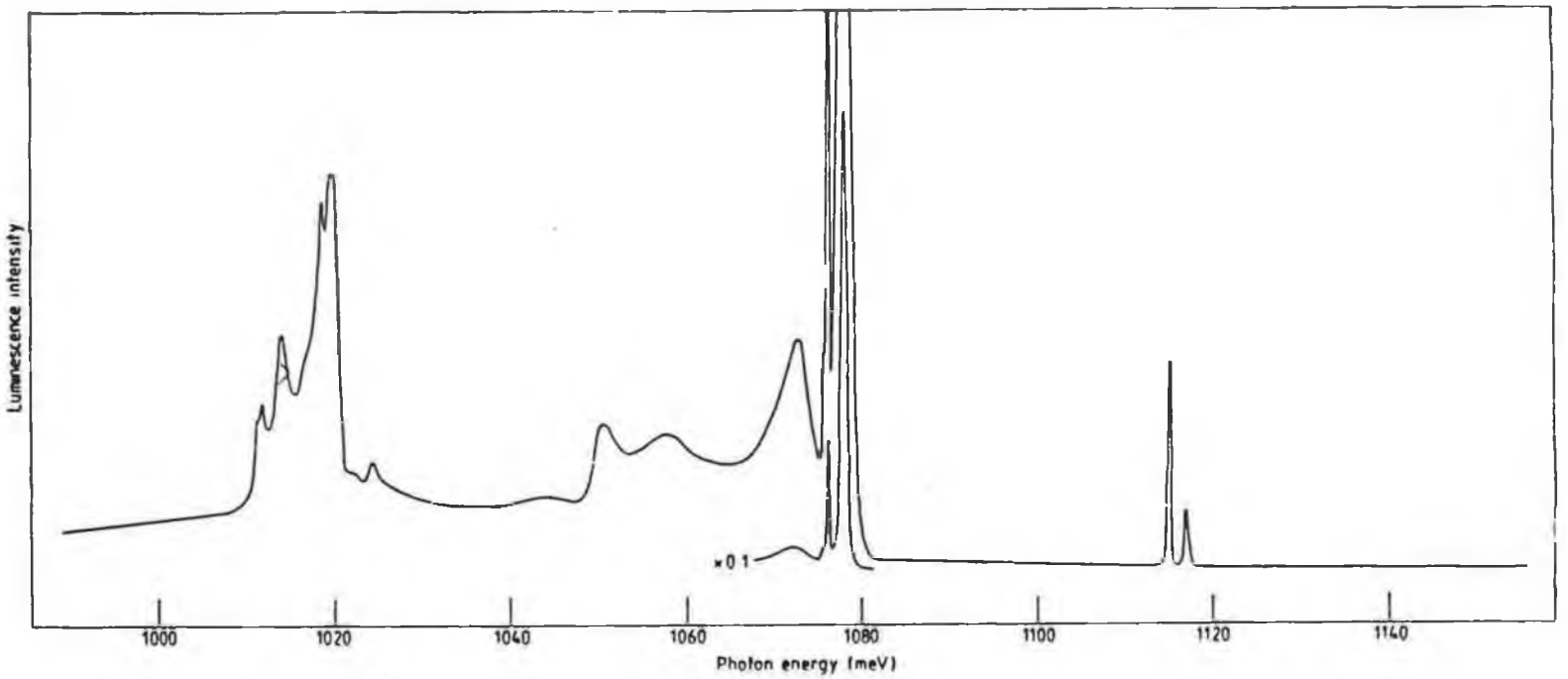

Fig 2.1 : Photoluminescence spectrum of Si:Be at 7K.
The no phonon lines of the Be IBE are centred around 1.077 eV. The higher energy system is due to another Ibe thought to be carbon related (Thewelt et al (1982))

(Taken from Henry et al (1981))

only reduces the degeneracy it also induces a partial mixing of the $|2,\pm1\rangle$ and the $|1,\pm1\rangle$ states thereby allowing transitions from the $|2,\pm1\rangle$ level to the ground state.

Given the level structure described above the observed temperature dependence of the luminescence can be explained as follows. The strong broad A line is taken to be an unresolved doublet of allowed transitions from the $|1,0\rangle$ and the $|1,\pm1\rangle$ states. This line is frozen out at the lowest temperature. The B line is due to the partially allowed transition from the $|2,\pm1\rangle$ state. Its intensity falls with increasing temperature as the population of the J=1 states increases and the A line becomes dominant. The B' line is attributed to the forbidden transition from the lowest energy state $|2,\pm2\rangle$ and is only observable at the lowest temperatures when the population of the other levels is negligible.

In Zeeman studies (Kiloran et al (1982)) the splitting of the lines is found to be simplest when the magnetic field is parallel to the $\langle 111\rangle$ crystal axis. This indicates that all the centres are oriented similarly for this field direction and therefore the axis of symmetry of the centre is $\langle 100\rangle$ as all $\langle 100\rangle$ directions are equivalent under a perturbation along a $\langle 111\rangle$ direction. Thus the luminescence is attributed to bound exciton recombination at an isoelectronic centre consisting of a Be-Be pair along a $\langle 100\rangle$ direction. The

photoluminescence lifetimes measured by Thewalt et al (1982) are very long; 480, 180, 4.6 microseconds for the B', B, A lines respectively. This supports the isoelectronic model of the centre. Using the measured values of the lifetimes the oscillator strengths were calculated and by comparison with the experimental values for the absorption coefficient an estimate of the concentration of the centre was made of 4×10^{16} cm^{-3}. This is as expected from the Be concentration. All that needs to be done to complete a classification of the centre is to determine whether it is donor or acceptor-like.

2.3 CLassification of the IBE

Phonon coupling is dominated by the most tightly held particle of the pair in the exciton, and electrons and holes couple differently. Holes can couple effectively with long range acoustic phonons and can induce phonon mixing of J=1 and J=2 states whereas electrons cannot. Thus even though the electronic level structure is very similar for excitons bound to donor and acceptor like centres the phonon sidebands are usually distinctive and can be used to ascertain the nature of an isoelectronic trap. Hopfield and Thomas (1966) who first divided IBE into donor and acceptor-like, conclude from work with ZnTe:O and GaP:Bi that the following differences should be present between the sidebands of the two types of IBE. For acceptor-like IBE the sidebands of the A and B lines should be

more or less identical as both will couple with the lattice in a similar way. As the B line represents a forbidden transition (from J=2 to J=0) the total emission from B is much less than that from A. For donor like IBE the A and B phonon wings will be different as the B sideband is derived from phonons that cross-couple B to A and the overall intensity of the B emission relative to that of the A will be increased. Also the zero phonon B line, as it is forbidden, will be very weak in comparison to its phonon sideband. These differences are clear in the spectra of ZnTe:O, an acceptor-like IBE, and GaP:Bi, a donor-like IBE, shown in figure 2.3.

Henry et al (1981) concluded that the phonon sideband of the forbidden B' line, seen in the 2 K spectrum, is due to cross-coupling with the A states. Their reasons were that it is different from both the A and B sidebands, seen at 13 K and 9 K respectively, which are very alike and in particular because of the strength of its low energy acoustic phonon band. As described by Hopfield et al this implies that the hole dominates the phonon interactions and therefore the centre is an isoelectronic donor. However the identification was only tentative as the absorption spectrum of the exciton, which appears to be a perfect hydrogenic series, could not be matched to a donor system despite extensive efforts by Henry (1982).

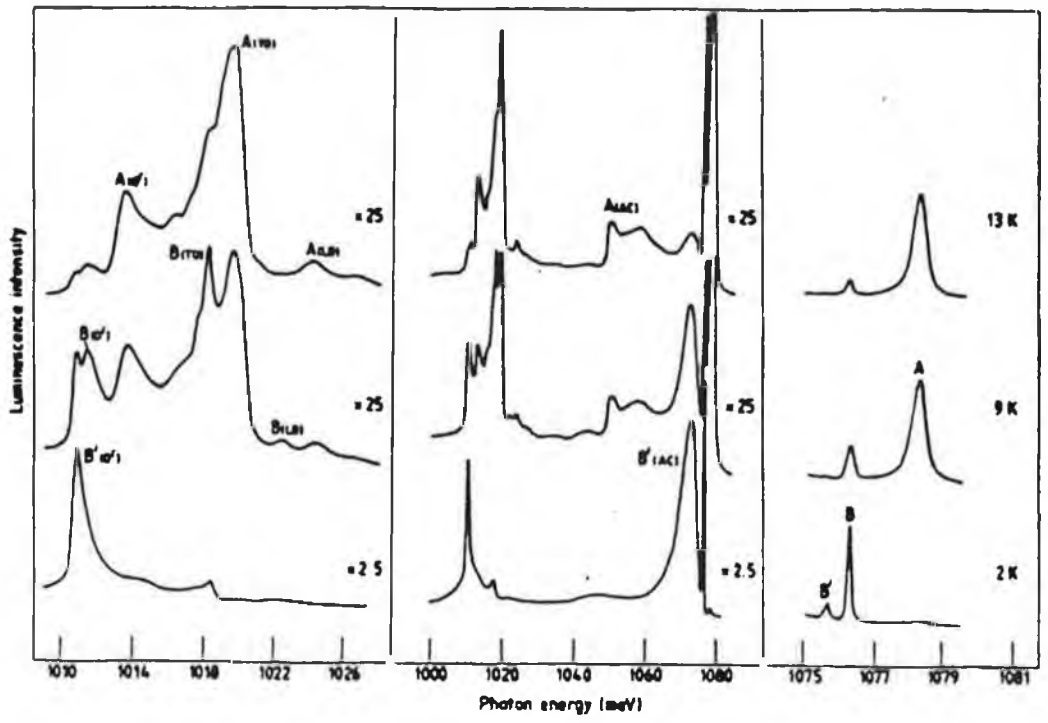

Fig 2.2 : Details of Si:Be photoluminescence at different temperatures. The no-phonon lines, showing thermalisation, and part of the phonon assisted sidebands are shown on either side of the full spectra.

(Taken from Henry et al (1981))

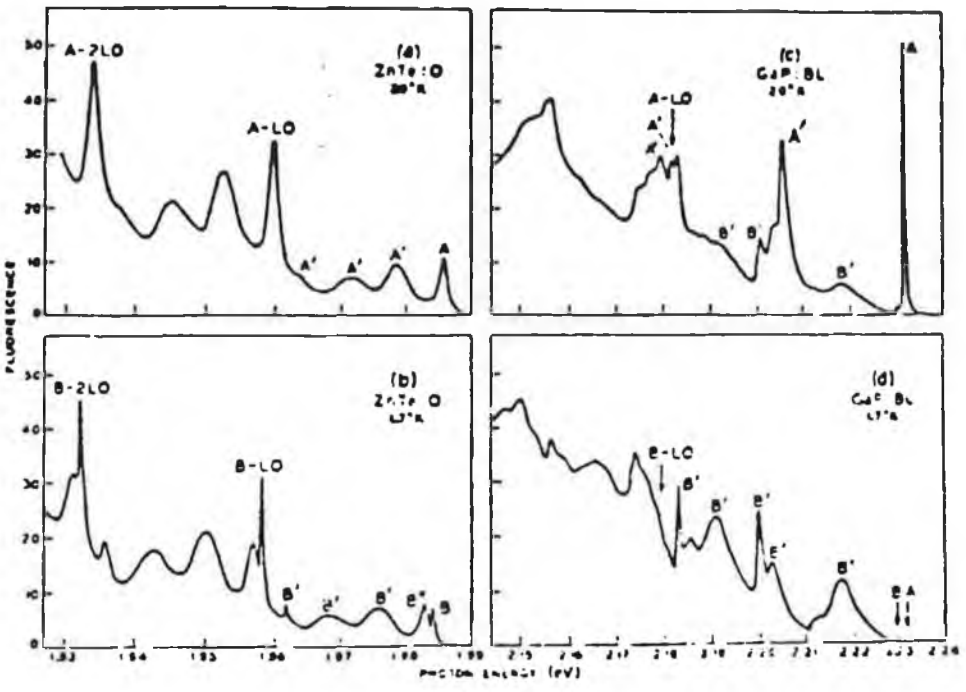

Fig 2.3 : The flouresecent spectra of ZnTe:O and GaP:Bi at 20 and 1.7K
(a) and (b) ZnTe:O, at 20k only the A spectrum is seen and at 1.7K only the B. Apart from the sharpness of the B line and the extra phonon wing B* the spectra are very similar merely being shifted by the A-B seperation (≈1.6meV).
(c) and (d) Gap:Bi, the A and B spectra are quite different. In particular the no-phonon B line is extremely weak compared to its phonon wings as it decays predominantly via phonon interactions which crosscouple A and B.

(Taken from Hopfield et al (1966))

More recently the far infra-red absorption spectrum of the Be related IBE has been recorded (Labrie et al (1984)) showing transitions between the ground state of the exciton and its odd parity excited states. It is found that the odd parity excited state spectrum of the boron acceptor in silicon, if shifted to lower energy by 3 meV, matches that of the Be IBE exactly, see figure 2.4. Comparison of the even parity excited states, as recorded by near infra-red spectroscopy, with those of the boron acceptor also gives good agreement when the 3 meV binding energy difference is included. Labrie et al identify the centre as an isoelectronic acceptor arguing that the sideband structure of the B' line is not as different from that of the A line as it may first appear as all the peaks of the B' sideband may be seen in the A sideband, with the exception of its low energy acoustic sideband. Thus it can be explained in terms of a weakly bound hole as would be present for an acceptor-like centre.

2.4 Conclusion

The purpose of the work described here is to try to determine conclusively the nature, whether donor or acceptor like, of the Be isoelectronic centre by means of a uniaxial stress analysis of the absorption spectrum of the bound exciton.

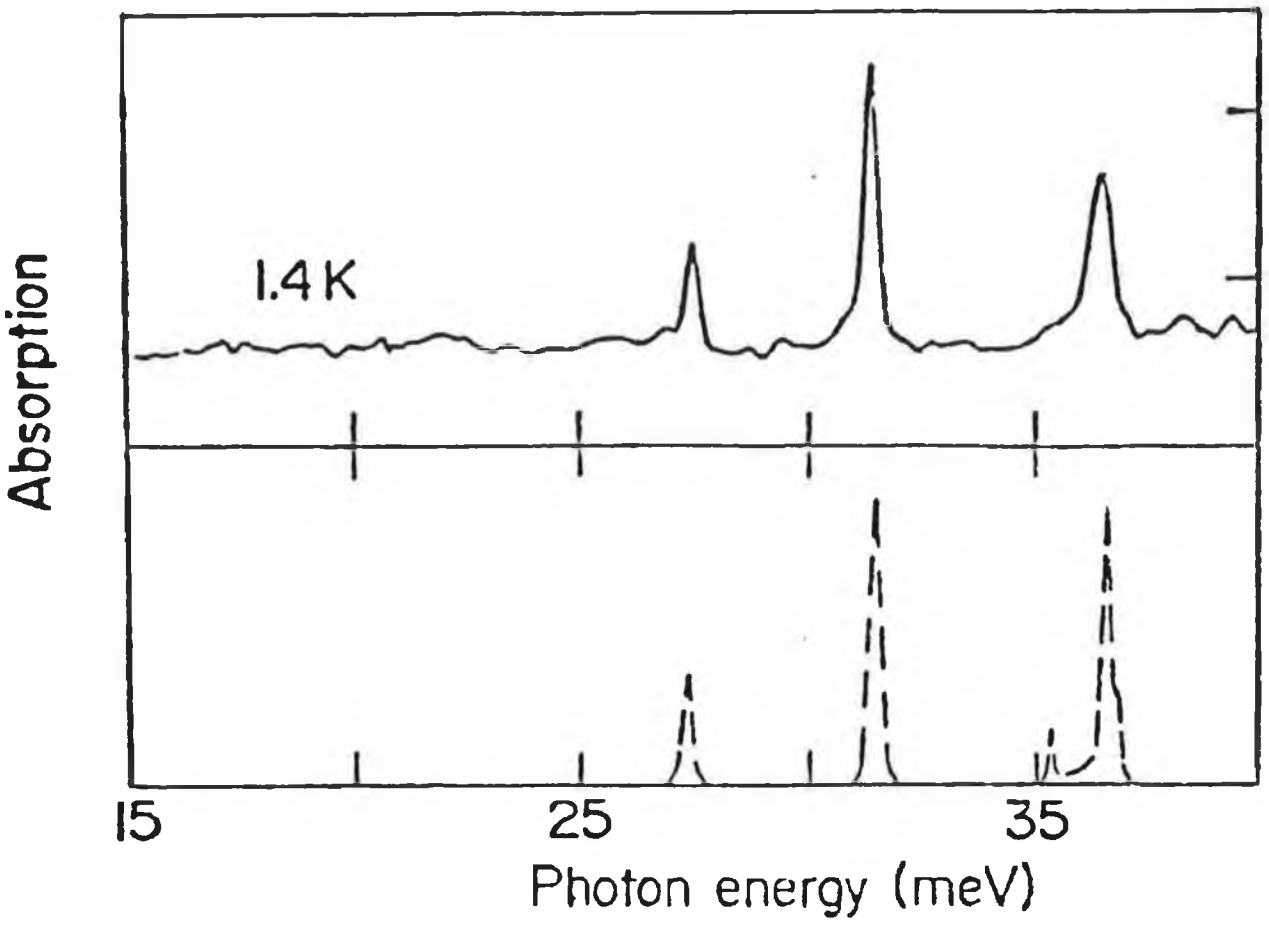

Fig 2.4 : Comparison of the Si:Be IBE and B acceptor absorption spectra.
(a) Induced absorption spectrum of the Be related IBE at 1.4K. Above band gap radiation was used to create the exciton in its ground state.
(b) The FIR absorption spectrum of the boron acceptor shifted by 3 meV.

(Taken from Labrie et al (1984))

CHAPTER 3

Experimental Methods

3.1 Introduction

The energy of the exciton states of interest is approximately 1.1 eV and therefore the corresponding transitions lie in the near infra-red. Because of this small binding energy the exciton will dissociate thermally unless the samples are cooled. Also thermal broadening of the absorption lines at room temperature would be such that they would be impossible to observe . For these reasons we worked at liquid nitrogen temperatures and even then some of the closer lying transitions could not be resolved. Working at low temperatures complicated the design of the stress apparatus necessitating the evacuation of the system to reduce thermal conduction . The presence of strong water vapour absorption lines in the wavelength region under investigation and weak absorption of some the stress split components made them very difficult to resolve. The experimental system developed to record the spectra and overcome these problems is described below.

3.2 General

Absorption spectra of silicon doped with beryllium under uniaxial stress were recorded at 85K. The features of interest lie in the wavelength range 11000 A° to 12000 A°. Three different samples, each roughly 2 X 4 X 12 mm, cut so that the long axis of each was oriented along one of ⟨100⟩, ⟨111⟩, and ⟨110⟩ crystallographic axes, were used. A block diagram of the apparatus used is given in figure 3.1.

The samples were prepared by evaporating a thin layer of Be onto a face of a number of rectangular pieces about 2 mm in thickness of high-resistivity zone refined Si (Hoboken 20 kΩcm). The pieces were placed in pairs, with the Be coated faces together, in rectangular tantalum boats and heated to 1300°C for 10 min to form a Si:Be eutectic alloy. They were then kept at 1000°C for roughly an hour to allow diffusion of Be from the eutectic. They were then sawn apart, lapped and etched in a 10% solution of HF in HNO_3.

The light source used is an Optronics 200 W tungsten filament lamp powered by an Optronics model 65 constant current source which delivers a steady 6.5 amps ensuring a stable incident intensity for absorption measurements. The light transmitted by the sample is collected by the aspheric lens L2 and focused on to the entrance slit of the monochromator by the biconvex lens L3.

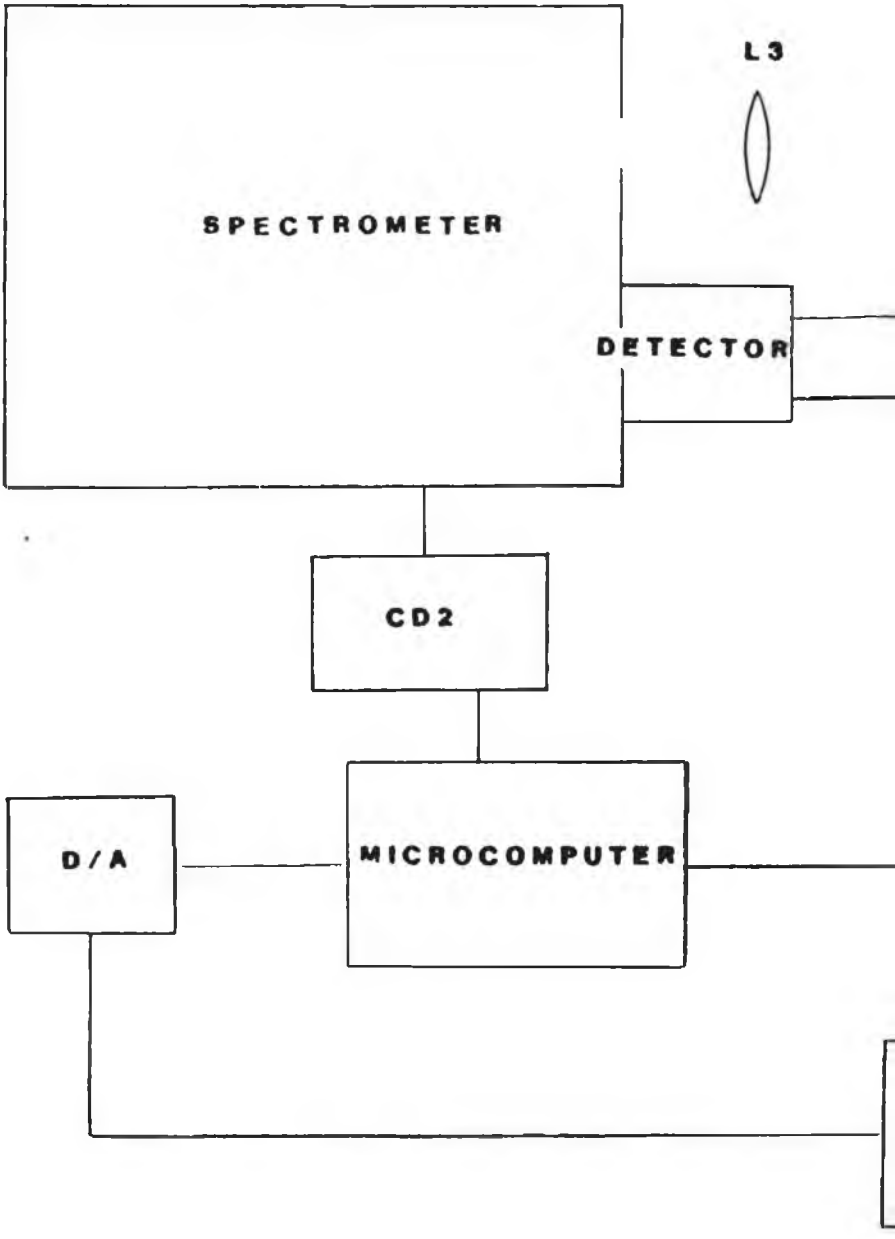
L3
SPECTROMETER
DETECTOR
CD2
D/A
MICROCOMPUTER

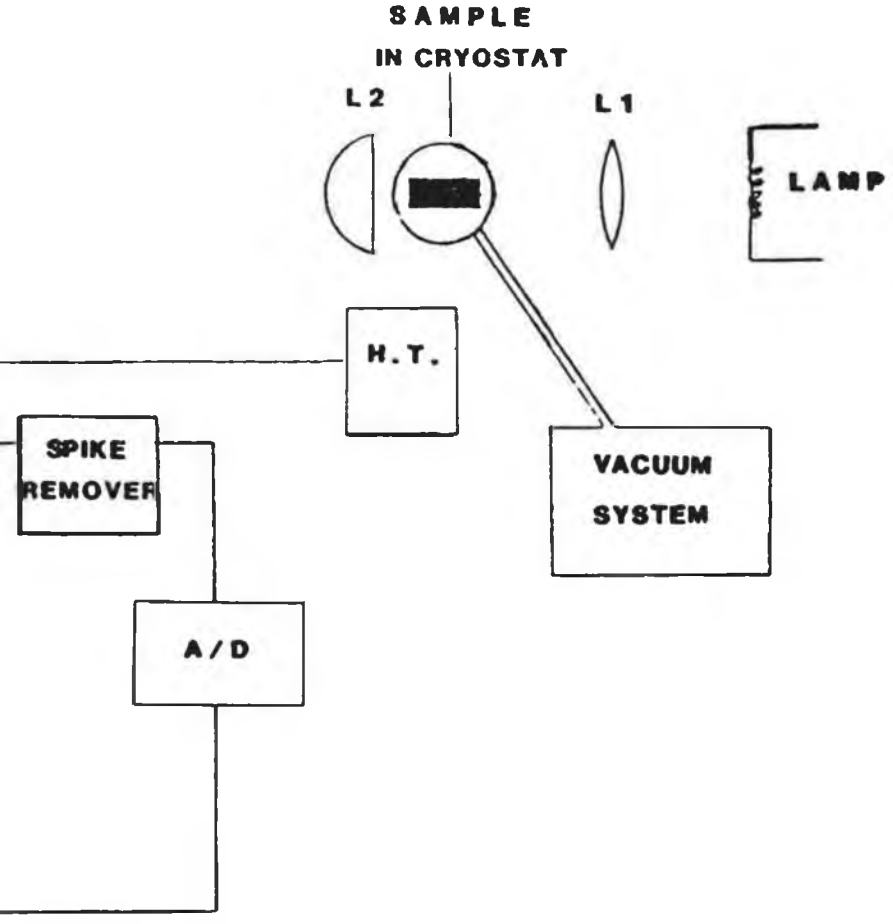

Fig 3.1 : Block diagram of apparatus.

The samples must be cooled to prevent dissociation of the exciton and to reduce thermal broadening of the lines. We achieved a temperature of 85K by placing the samples in a stream of cold nitrogen vapour obtained by boiling liquid nitrogen in a cryostat by passing a current of about one amp through two 25 watt resistors which were dangled in the liquid. The rate of production of the vapour, and thus the rate of cooling, is controlled with a variac. The temperature of the sample is measured using a copper constantan thermocouple in good thermal contact with the sample and with a reference junction at 77 K. The sample holder is surrounded by a double walled glass chamber, a Maeda (1965) type cryostat shown in figure 3.2, which is evacuated to minimize heating by conduction and silvered on the inside (except in light path) to reduce radiative heating of the sample. Condensation on the unsilvered glass in the light path was removed using hot air from a blower. The procedure for silvering the glass is as follows: Two solutions were prepared. Solution A was made by dissolving 6 g of $AgNO_3$ in 100 mls of deionized water and then slowly adding NH_4OH until a precipitate was formed and then just redissolves. This solution was then made upto 500 mls with deionized water. Solution B was made by adding 0.5 mls of concentrated HNO_3 to a solution of 8 g of sucrose in 150 mls of water and boiling for 2 minutes. After cooling 150 mls of methanol were added. These two solutions were mixed in the ratio A:B of 10:1. This final solution was poured into

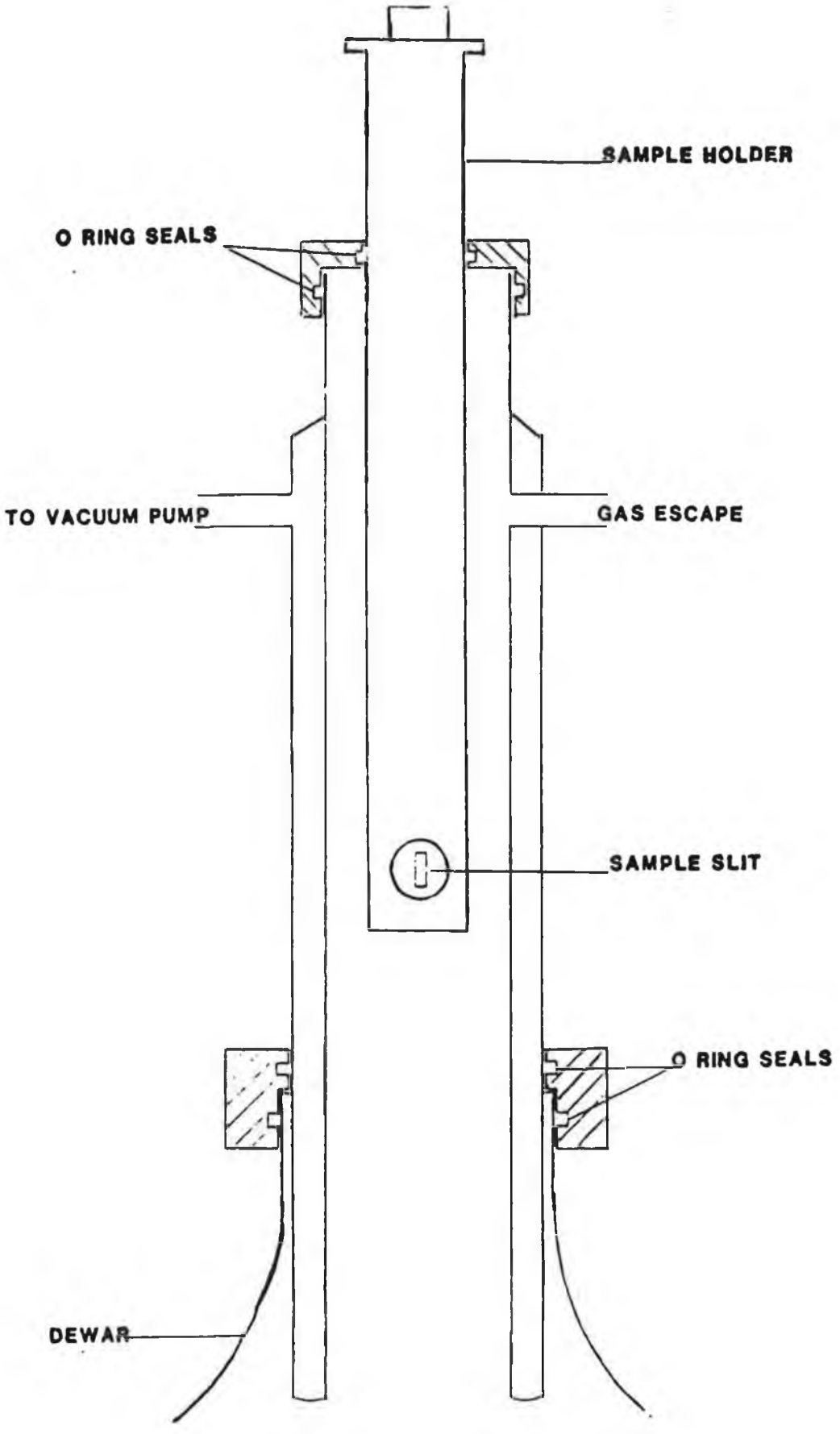

Fig 3.2 : Cryostat
Cold nitrogen vapour produced in the dewar flows past the sample, cooling it, and out through the escape vent.

the vacuum space of the cryostat and allowed to stand for 24 hours by which time the silvering was complete.

The spectrometer used is a Spex 1704 one metre Czerney Turner with a grating ruled at 600 lines/mm and blazed at 1.2 microns. The grating motors are controlled by a Compudrive CD2 microprocessor based unit which provides several modes of operation and a digital readout of the wavelength selected. The mode used is called the "Triggered Burst Scan" mode in which one sets a starting and a finishing wavelength and a wavelength increment; each time the control unit receives an external trigger pulse it moves the grating through one wavelength increment from the starting value until eventually the final wavelength is reached. 100 micron slits were used which give good resolution, about 0.25meV compared with linewidths of roughly 4 meV, and a strong signal.

The detection system used is a North Coast EO-817 cooled Germanium Detector. This consists of a P.I.N. diode fabricated from ultra high purity germanium and a low noise preamplifier. The diode and the F.E.T. first stage of the amplifier are kept at 77K by means of a liquid nitrogen dewar built into the system. It takes about 1.5 hrs. to cool the detector and the hold time of the dewar is roughly 10 hrs. The result is that the detector gives high sensitivity (Responsivity 4×10^8 V/W) extremely low noise performance in the region 0.8 - 1.8 microns. The diode is reverse biased

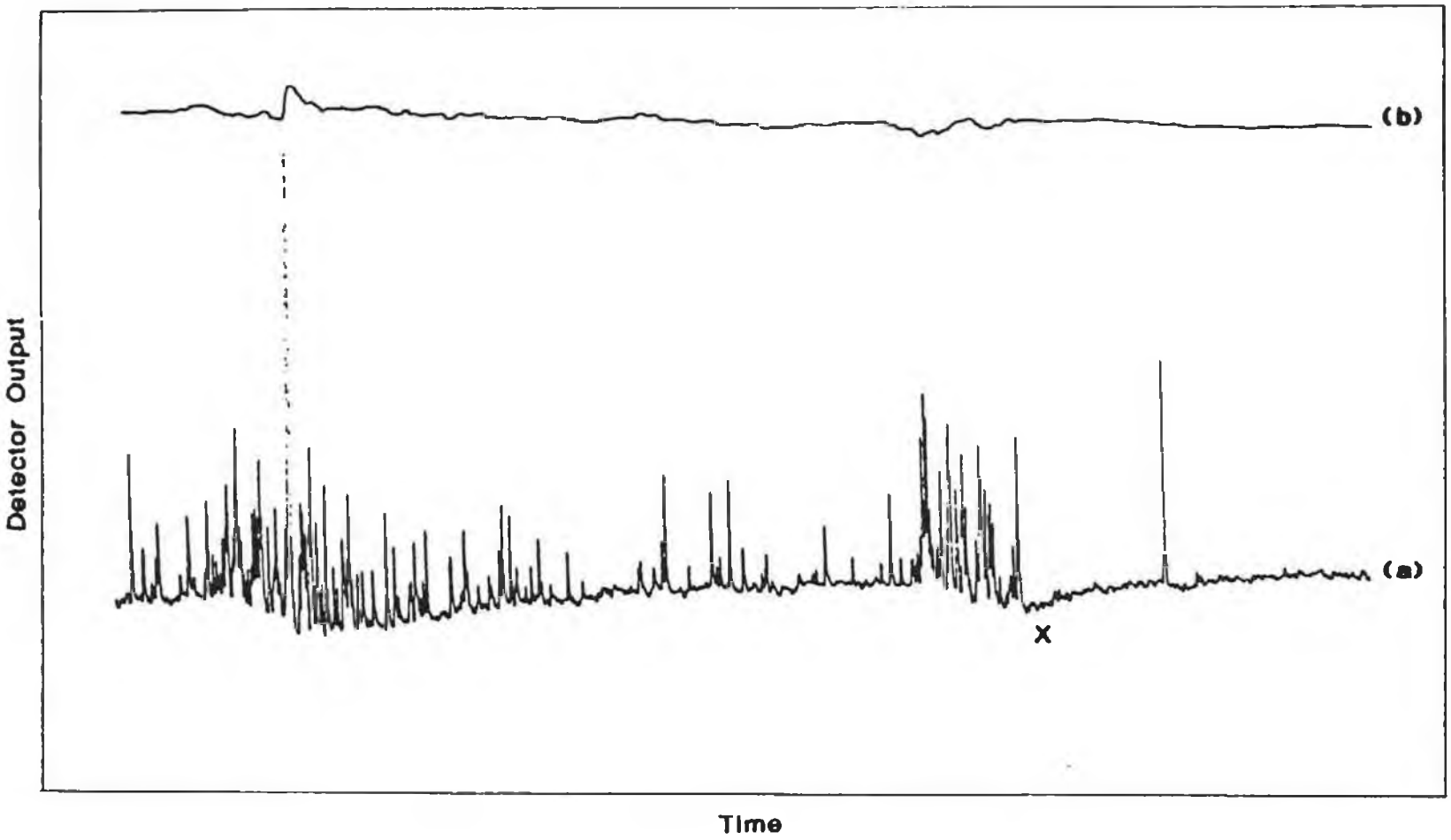

Fig 3.3 : Radiation spike removal.

(a) Output of the detector showing spikes caused by a γ source nearby and a decrease in their number when the source is removed (at X).

(b) Output of detector "cleaned" by the spike removal unit showing near perfect supression of the pulses.

with a large negative voltage, -100 V was used, and has a quiescent dark output of -0.8 to -1V,the level drifting down gradually over a period of several hours.

In fact the system is so sensitive that environmental radiation causes large spikes on the output. To overcome this problem an electronic spike removal unit was built based on a circuit developed by Collins and Jeffries (1982). The circuit works by passing the output of the detector through a sample and hold chip; the output is also differentiated and used to trigger the sample and hold amplifier. When a spike appears on the output of the detector it produces a large differentiated signal causing a monostable to trigger which in turn makes the sample and hold to go into hold mode, freezing out the spike. The hold time is varied by changing the length of time for which the monostable triggers. The sensitivity can be altered by changing the amplification of the differentiated signal used to trigger the monostable. Figure 3.3 shows clearly the presence of these spikes, a dramatic increase in their number when a gamma ray source is brought near the detector, and the elimination of the spikes by the unit. Variable gain, smoothing and d.c. backoff facilities were also included in the circuit. A circuit diagram is given in figure 3.4 and P.C.B. layout of the spike remover is included in appendix 1.

The signal from the detector is fed through an analog to

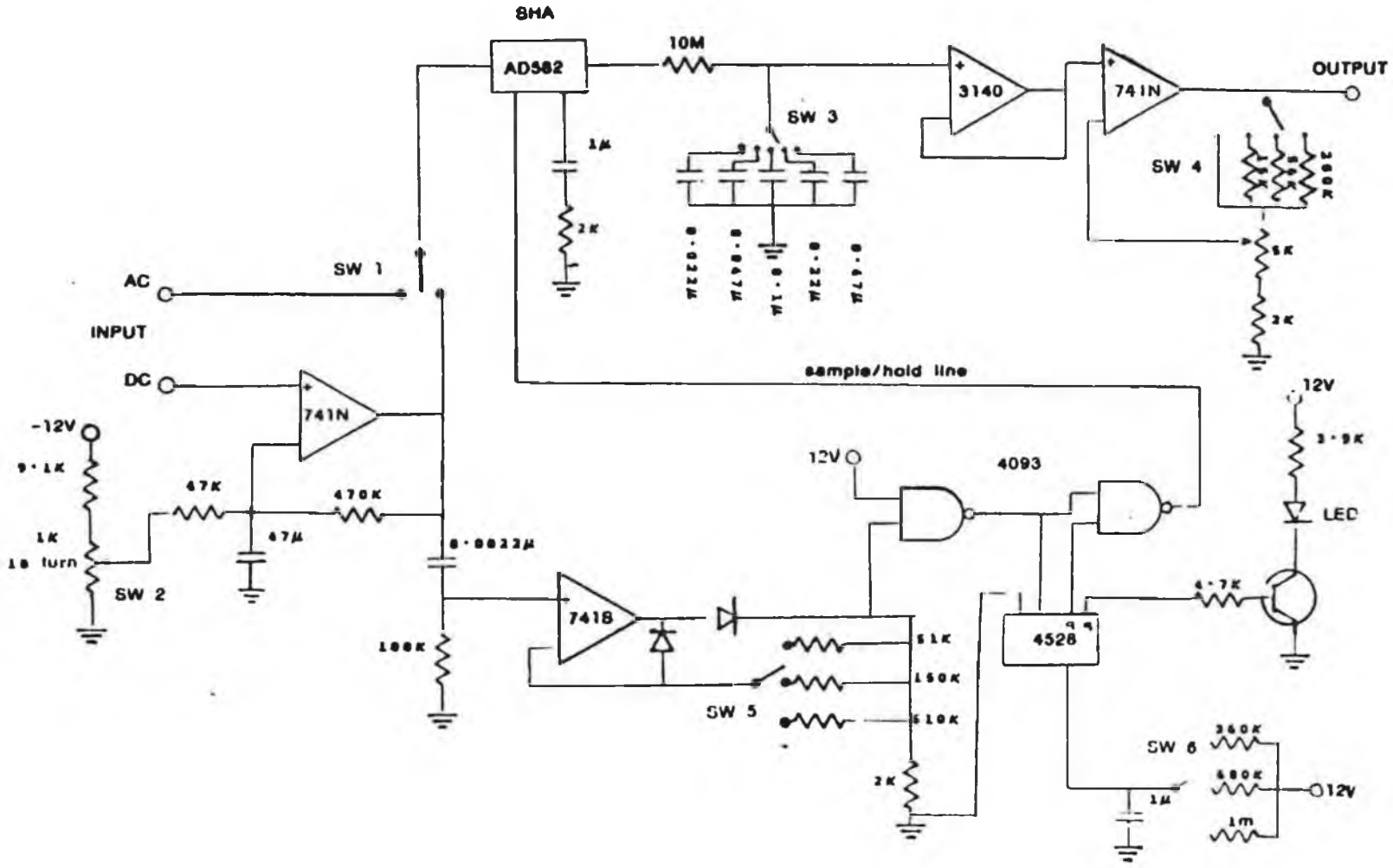

Fig 3.4 : Circuit diagram of spike removal unit
Switch 1 (SW 1) selects direct or chopped input
Switch 2 (SW 2) variable d.c. backoff
Switch 3 (SW 3) selects smoothing
Switch 4 (SW 4) coarse gain select
Switch 5 (SW 5) sets sensitivity
Switch 6 (SW 6) sets holdtime

digital converter to a microcomputer for recording and processing. Initially an Acorn Atom was used but as this proved unsatisfactory it was later replaced with a BBC model B. The computer controls the spectrometer and records the spectra as follows; it sends a trigger pulse to the CD2 causing the spectrometer to move to the next wavelength, waits until the wavelength has been selected, reads in the output of the detector through the A/D, averages it and stores it in an array and then sends another trigger pulse to the CD2. Due to memory constraints the maximum number of data points that could be recorded for each spectrum was 256. A wavelength increment of 2.5 A°was therefore needed to cover the whole region of interest. After processing the final spectrum is sent via a digital to analog converter to a Houston Instruments Omniscribe chart recorder for plotting.

3.3 Stress Rig and Sample Holder

Stress is applied to the sample using a lever apparatus and lead weights as illustrated in figure 3.5. The stress is transmitted to the sample, which is held between 2 stainless steel pistons, via a hollow, cylindrical push rod. The load is carried by the outer tube which is held by the support frame. The fact that the tubing is long hollow and thin-walled helps to reduce heat conduction to the samples. The major problems in mounting the sample are getting it steady so that it doesn't slip under stress and preventing

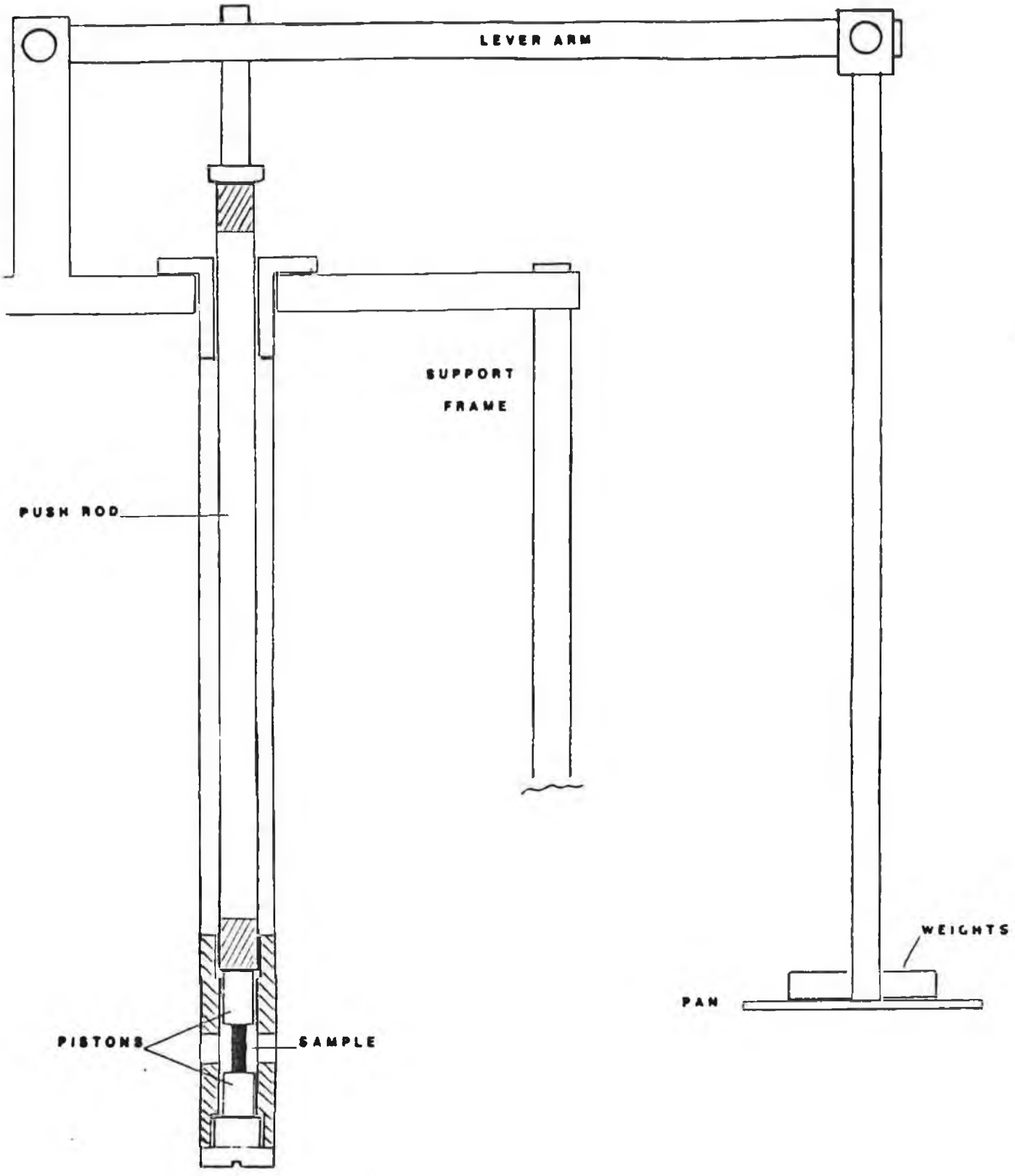

Fig 3.5 : Stess rig
The sample is enclosed in the cryostat as illustrated in Fig. 3.2 .

stray light from getting past the sample. We overcome them by sticking the sample to the pistons with vacuum grease which hardens as it cools and by packing tissue paper around the sample which both steadies it and blocks stray light. There are three points of attachment for the weight pan to the lever arm allowing three different multiplication factors of roughly 5, 8 and 10. The system was calibrated by placing a load cell (Bofors Electronik KRA-1) under the load point and hanging masses on the pan. The load cell itself had previously been calibrated and found to be perfectly linear. Thus it is possible to convert from the mass on the pan, knowing the point of attachment, to the force acting on the sample. The area of the samples being roughly 7 mm^2, a mass of 30 kg hanging from the lever at the multiplication by 10 point gives a pressure of 440 MPa on the sample whereas 500 g at multiply by 5 point gives 27 MPa. The weight of the pan and lever have been included in both cases.

3.4 Signal Processing

The spectral region in which the exciton absorption features lie is also an area of strong atmospheric water vapour absorption. This absorption consists of a large number of sharp narrow lines overlapping the exciton lines and of roughly the same intensity as shown in figure 3.6(a). As we do not have access to a suitable dual beam spectrometer it was decided to use the microcomputer to remove this interference.

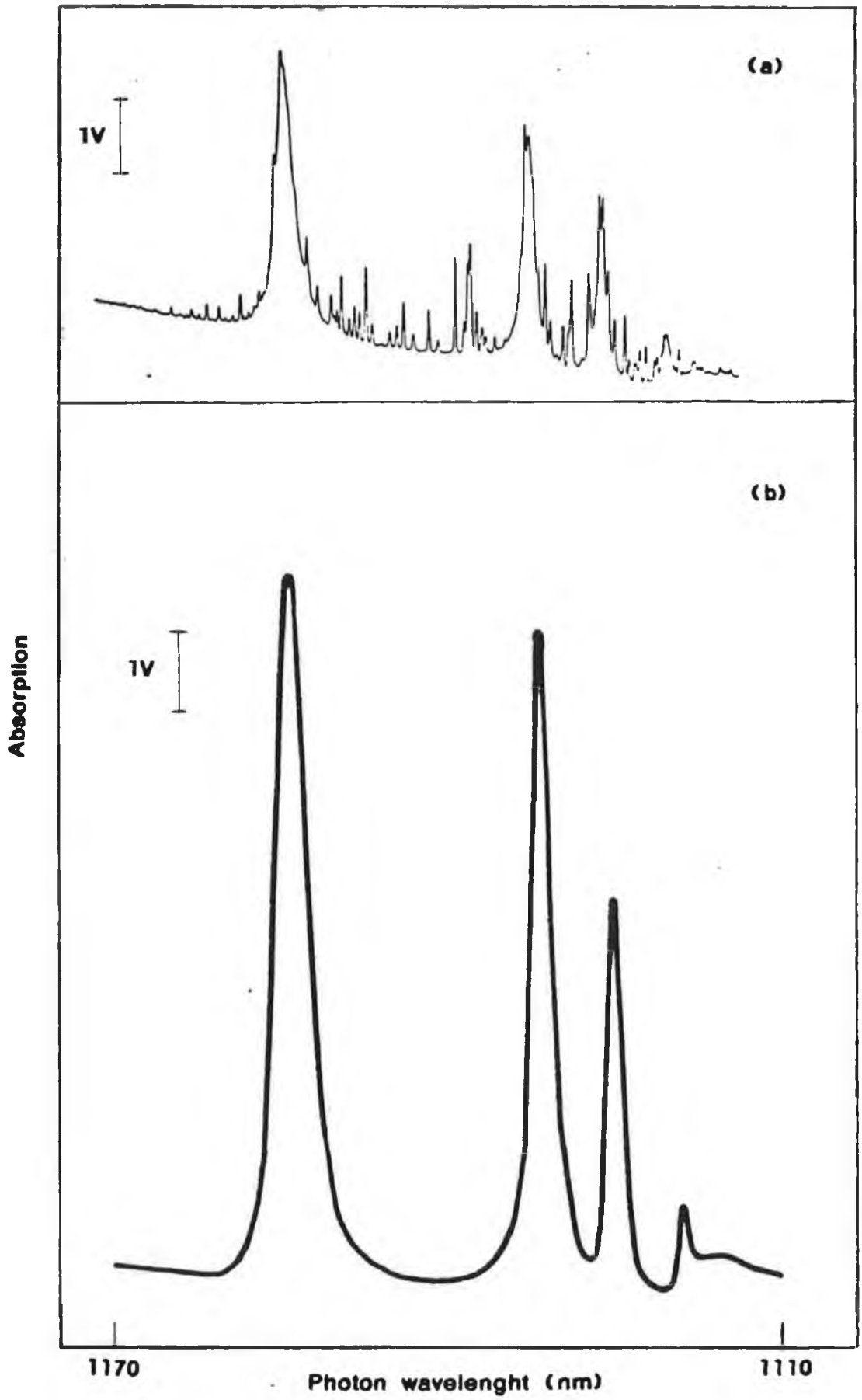

Fig 3.6 : Spectrum processing by microcomputer.
(a) Asorption spectrum of Si:Be with overlapping water vapour features.
(b) Final enhanced spectrum produced by program (same scale).

The technique developed is to record two spectra. The first, called the signal, is the absorption spectrum of the silicon sample including the water vapour lines while the second, called the background, is obtained by removing the sample and passing the radiation through the same path in air so that this spectrum contains the water vapour absorption at the same strength. When the sample is removed from the path the light intensity reaching the detector increases dramatically. To reduce it to a level similar to that of the signal spectra neutral density filters are inserted in the light path. The signal spectrum is normalized with respect to the background to remove the water vapour features by calculating the following quotient at each data point;

$$\frac{\text{Background - Signal}}{\text{Background}}$$

This quotient, while it is not the absorption coefficient, is related to it and has the same general shape. It is this that we plot as our final spectra. This technique also removes the need to calibrate the system as it automatically compensates for any variation with wavelength in the output of the lamp, the response of the spectrometer or the sensitivity of the detector.

Thus in theory the water vapour lines can be removed completely but in practice complications arise. A change in

humidity while taking spectra means that the strength of water vapour lines changes and new background spectra must be taken repeatedly. The water vapour lines are very narrow (F.W.H.M. < 2 A°) and consequently any deviation from complete reproducibility by the spectrometer when taking the two spectra can cause non-cancellation of a water vapour feature and introduce differential type positive going and negative going spikes. This is a major problem when working with a stressed sample as the stress split components of some of the lines are very weak, often weaker than the water vapour features, and can easily be lost. To overcome this we decided to reduce the strength of the water vapour absorption by lowering the concentration of water vapour in the light path. The majority of the light path, 4 m out of 5 m, is in the spectrometer so by reducing the humidity of the air inside it the strength of the water vapour lines is greatly reduced. This was done firstly by flushing the spectrometer with dry nitrogen and later by the more economical and convenient method of packing the spectrometer, which being light tight is more or less air tight, with silica gel. The spectra obtained using these improvements, see figure 3.6(b), proved satisfactory.

The program written to carry out the above procedure, a listing of which is given in appendix 2, also performs a number of other tasks. A flow chart is given in figure 3.7 . Initialization involves setting up the interface and defining

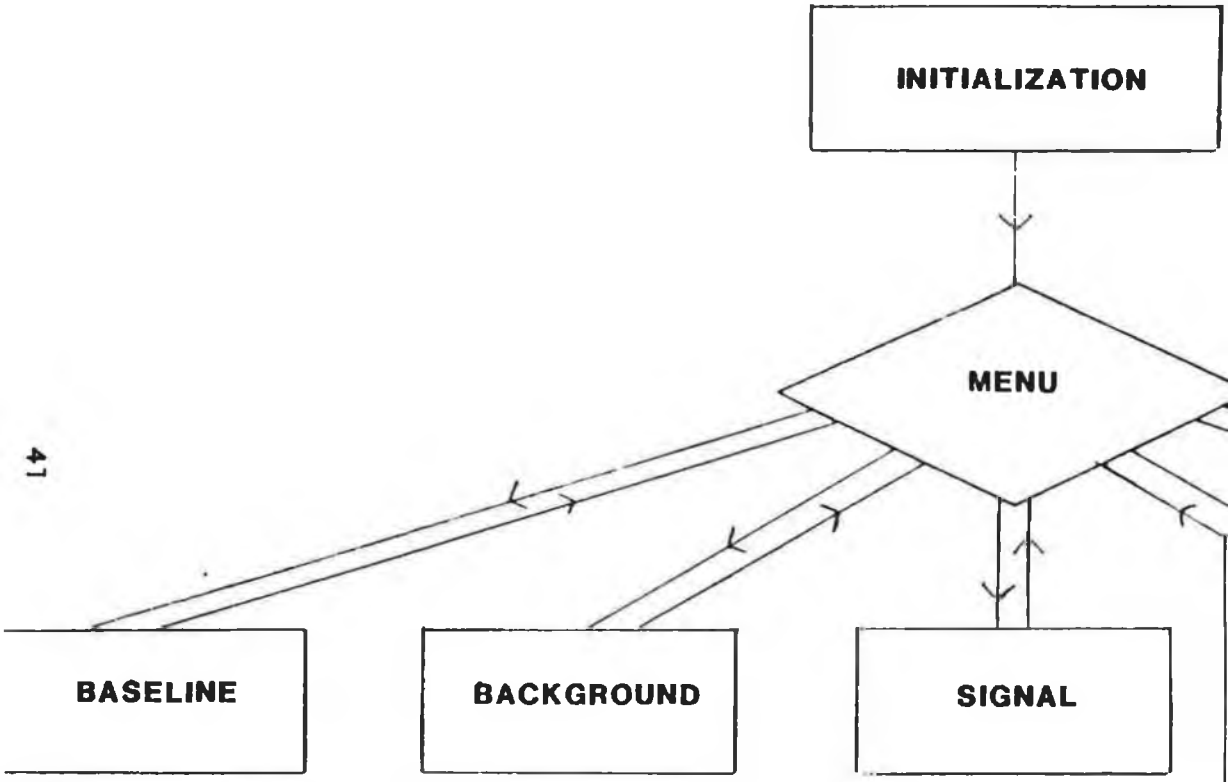

Fig 3.7 : Flowchart of program used to record spectra.
The normal sequence in which operations are performed is :
Baseline, Signal, Background, Remainder, Manipulate Cursor, Chart.
After each operation control returns to the menu.

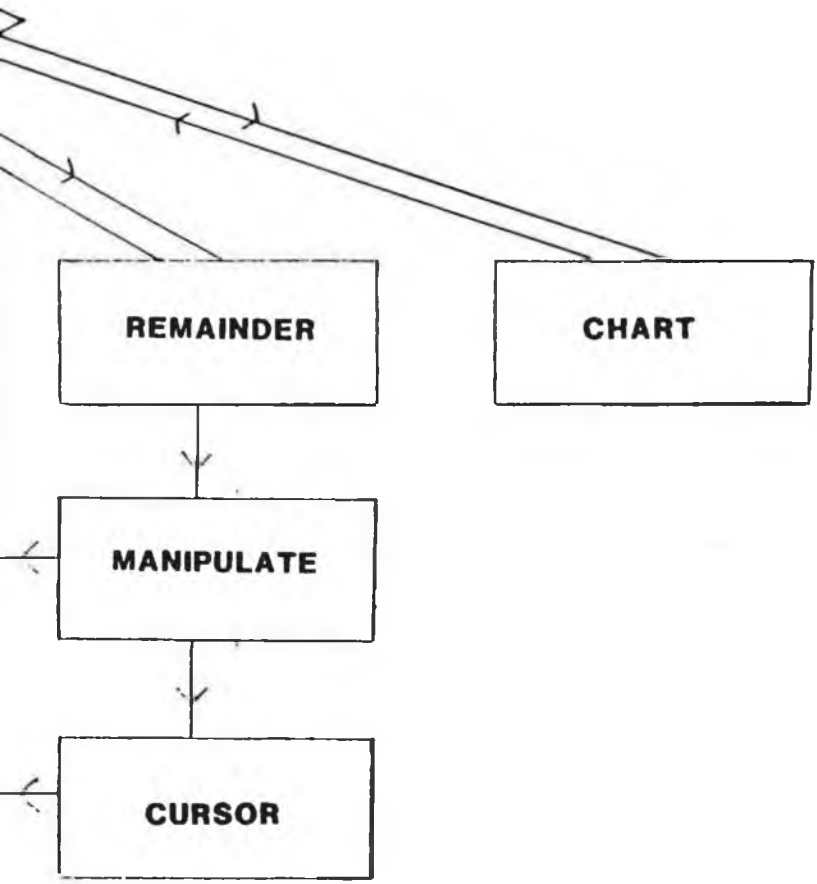
REMAINDER
CHART
MANIPULATE
CURSOR

the arrays needed in the program. The Menu allows one to select any of the five separate operations in the program. The procedure "Baseline" reads in the dark output of the detector and stores it to correct for it in all subsequent readings of detector output. The routine "Signal" reads the signal spectrum, stores it and plots it while controlling the spectrometer as described above. Before starting to record a spectrum a continually updated value of the detector output is displayed on screen enabling one to adjust the optics for a maximum signal. The routine "Background" is identical to "Signal" except that the spectrum is stored in a different array . The background is usually recorded after the signal as it must always be the larger of the two. The routine "Remainder" calculates the quotient, plots it with suitable scaling and smooths it digitally by making the value at each wavelength the weighted average of the value at that data point and the two points on either side. The exciton absorption features are very weak and thus the lines sit on top of a large residual light signal which is of no significance here. The procedure "Manipulate" therefore subtracts it and magnifies the portion of interest. There is also present a sloping background absorption due to the sample which slightly distorts the exciton lines. This too is removed in this procedure and the smoothed spectrum is then plotted. The final spectra thus produced contain only the features of interest greatly enhanced. The subroutine "Cursor" enables one to find easily the wavelength of the

maximum of an absorption line by moving a vertical line cursor across the spectrum displayed on the screen and printing the wavelength corresponding to its position. The procedure "Chart" outputs a spectrum through the D/A, with appropriate scaling, to the chart recorder.

CHAPTER 4

Results

4.1 Introduction

The experimental system and procedure having been finalized as described in chapter 3 stressed absorption spectra were recorded for a wide range of applied pressures. The stress split components of the higher energy lines are very weak and proved to be very difficult to resolve. As a result spectra had to be retaken repeatedly after adjustments had been made to maximize the signal. This was very time consuming as any change in the sample positioning required bringing the system back upto room temperature and then recooling it . The absorption lines of the <111> sample are considerably weaker than those of the other two samples, presumably due to lighter doping. The higher energy component of line 4 is extremely weak for all samples and consequently very difficult to follow under stress. This proved to be the major experimental difficulty but eventually, through perseverence, satisfactory data were obtained.

4.2 Results

The unstressed absorption spectrum of Si:Be at 85 K is shown in figure 4.1. It is essentially the same as that recorded by Thewalt et al (1982) at 2 K except the linewidths at 85 K are approximately four times those at 2 K, the weakest lines observed at 2 K are not detected at 85 K and the line centres are shifted to lower energy by roughly 3meV. The latter is related to the temperature shift of the band gap. The lines observed, numbered 1 to 4 in the diagram, are strong enough and sufficiently well resolved to study under stress. Line 1 corresponds to the electric dipole allowed A transition, i.e. to a J=1 final state, as seen in luminescence (Henry et al (1981)). The B lines present in luminescence are not seen in absorption. Lines 2,3 and 4 are transitions to excited states of the exciton.

Absorption spectra at 85 K were recorded over a range of stresses, upto 500 MPa, along each of the three axes ⟨111⟩, ⟨100⟩ and ⟨110⟩. The results are summarized in figures 4.2-4.4 which give sample spectra at different stresses showing the splitting patterns and in figures 4.5-4.7 in which the energies of the line centres are plotted as a function of applied stress. Line 1 splits into 3 components for each stress direction, line 2 doesn't split at all and lines 3 and 4 both divide into 2 components. It is clear that line 2 interacts with the low energy stress split component of line 3

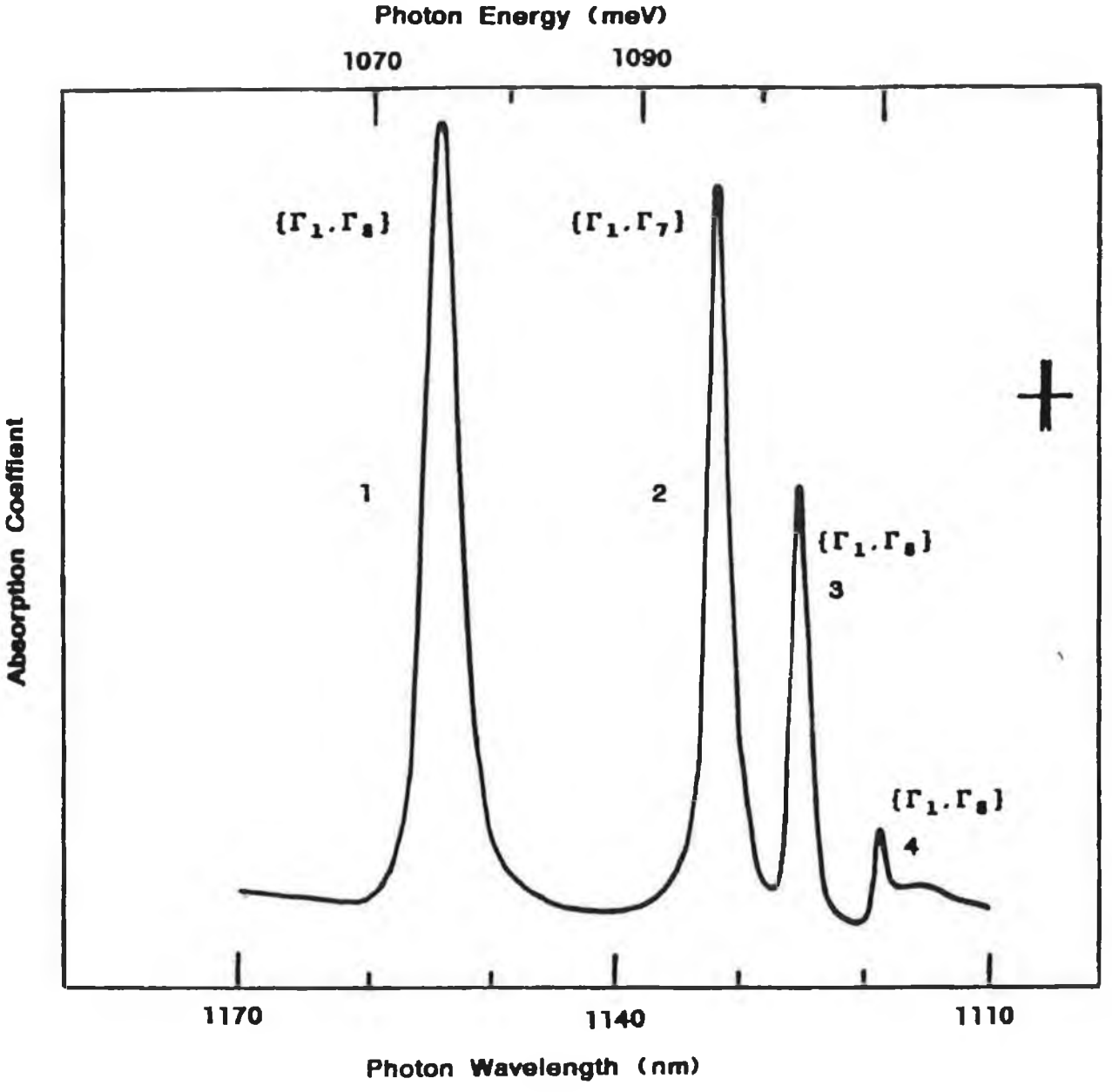

Fig 4.1 : The unstressed absorptions spectrum of Si:Be at 85K. The four lines are labelled according to the irreducible representations of the electron-hole pair which constitutes the exciton, after the model of Labrie et al (1984)

for all stress directions, as does the high energy component of line 3 with the low energy component of line 4. The labels on the components are explained in chapter 5.

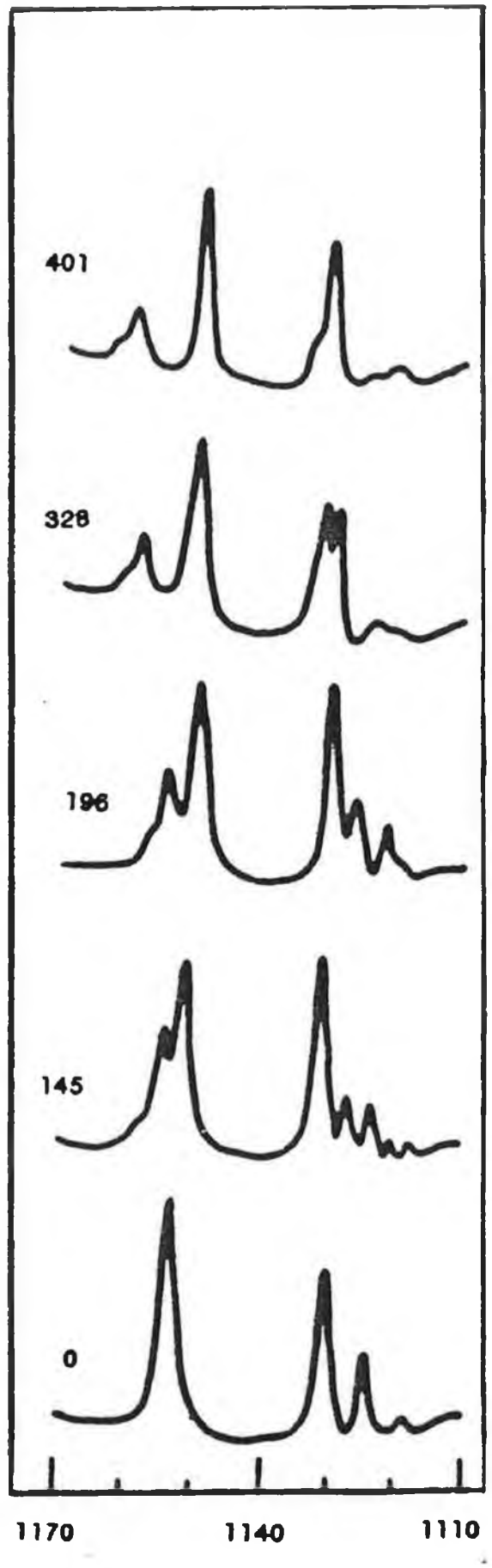

Fig 4.2 :
Absorption spectra of Si:Be for different stresses, given in MPa, along <111>.

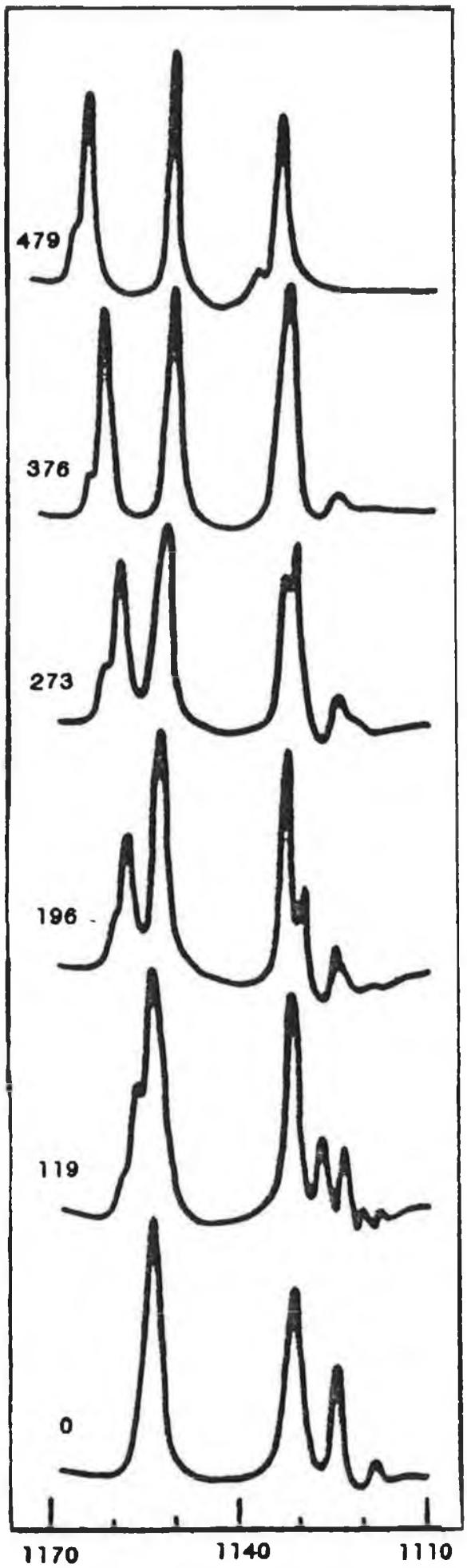

Fig 4.3 :
Absorption spectra of Si:Be for different stresses, given in MPa, along <100>.

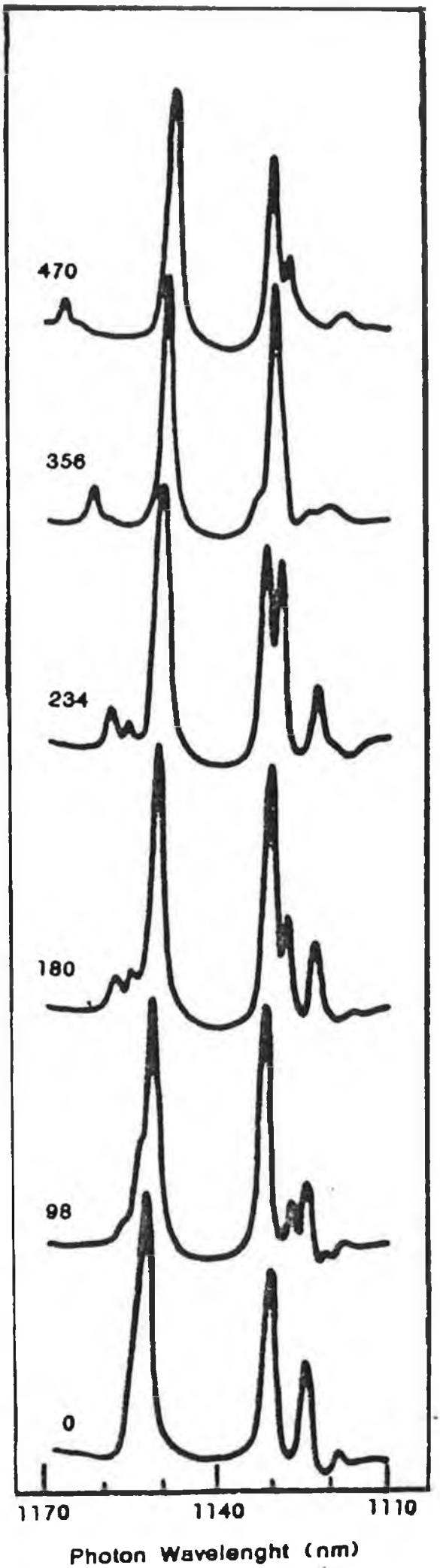

Fig 4.4 :
Absorption spectra of Si: Be for different stresses, given in MPa. along <110>.

Fig 4.5 : Stress splittings of the Si:Be no-phonon lines for stress along <111>

Components of line 1 are labelled using $|J, M_J\rangle$ notation while line 2 and components of lines 3 and 4 are labelled according to the irreducible representation of the exciton hole.

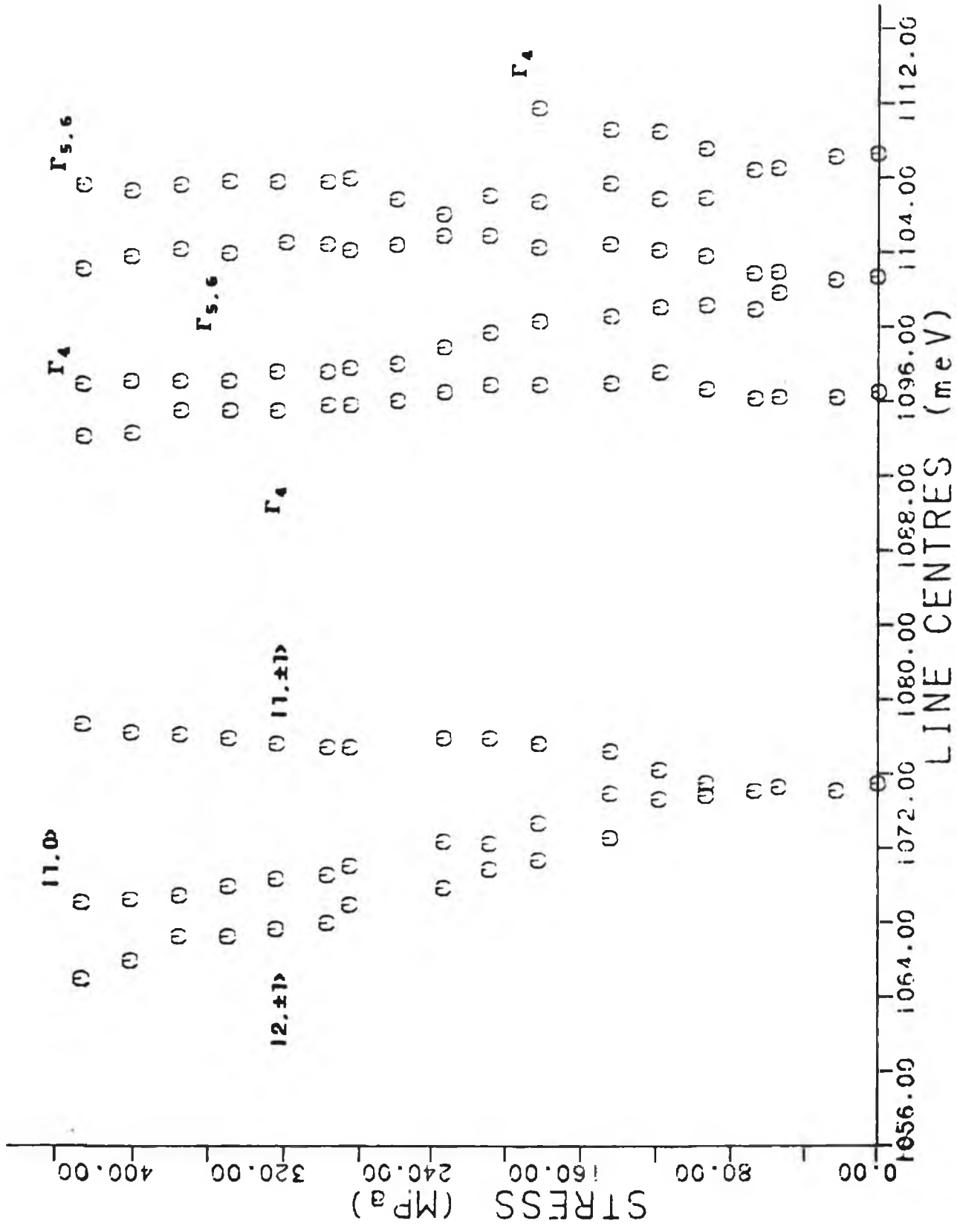

Fig 4.6 : Stress splittings of the Si:Be no-phonon lines for stress along <100>

Components of line 1 are labelled using $|J, M_J\rangle$ notation while line 2 and components of lines 3 and 4 are labelled according to the irreducible representation of the exciton hole.

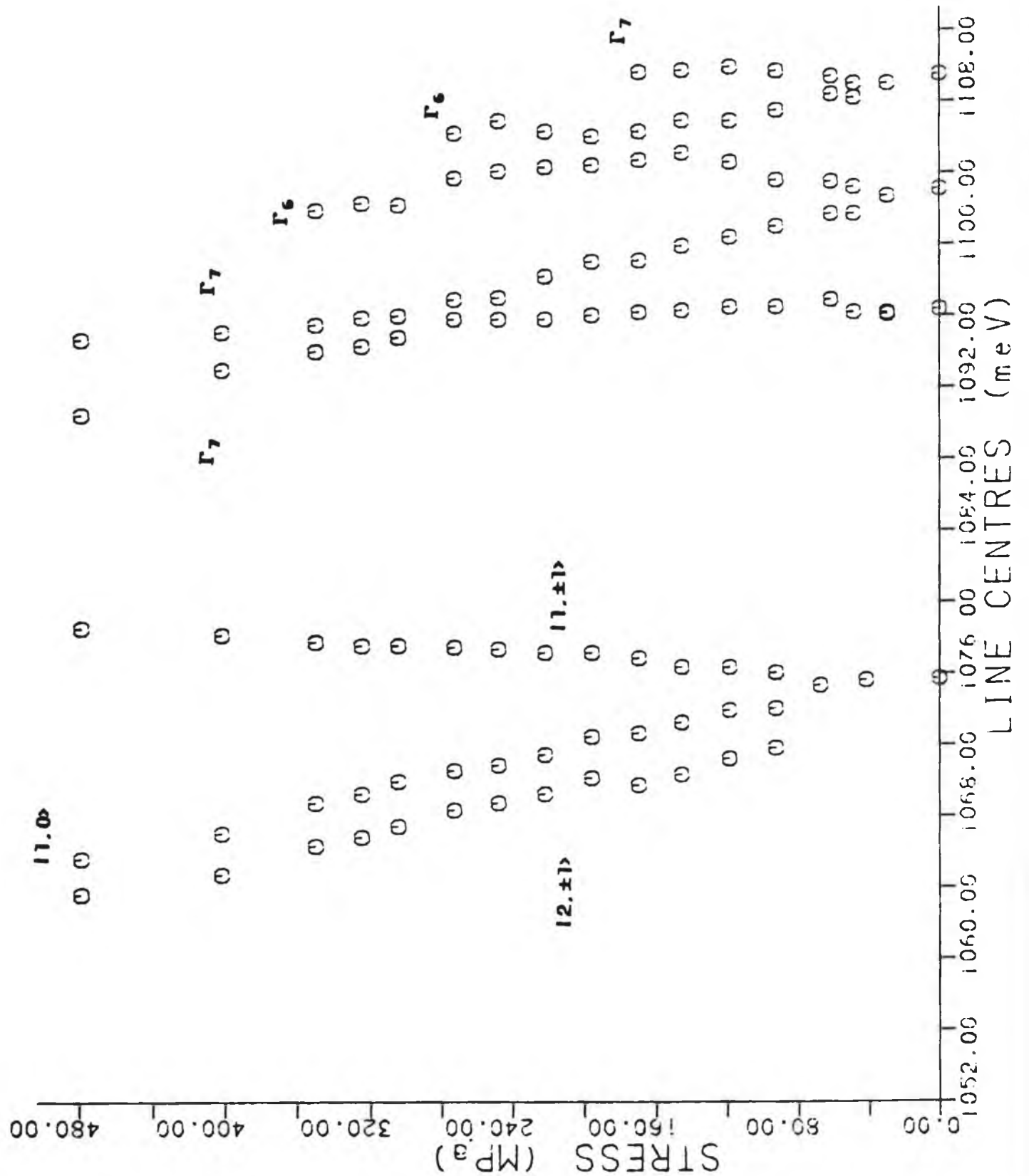

Fig 4.7 : Stress splittings of the Si:Be no-phonon lines for stress along <110>

Components of line 1 are labelled using $|J, M_J\rangle$ notation while line 2 and components of lines 3 and 4 are labelled according to the irreducible representation of the exciton hole.

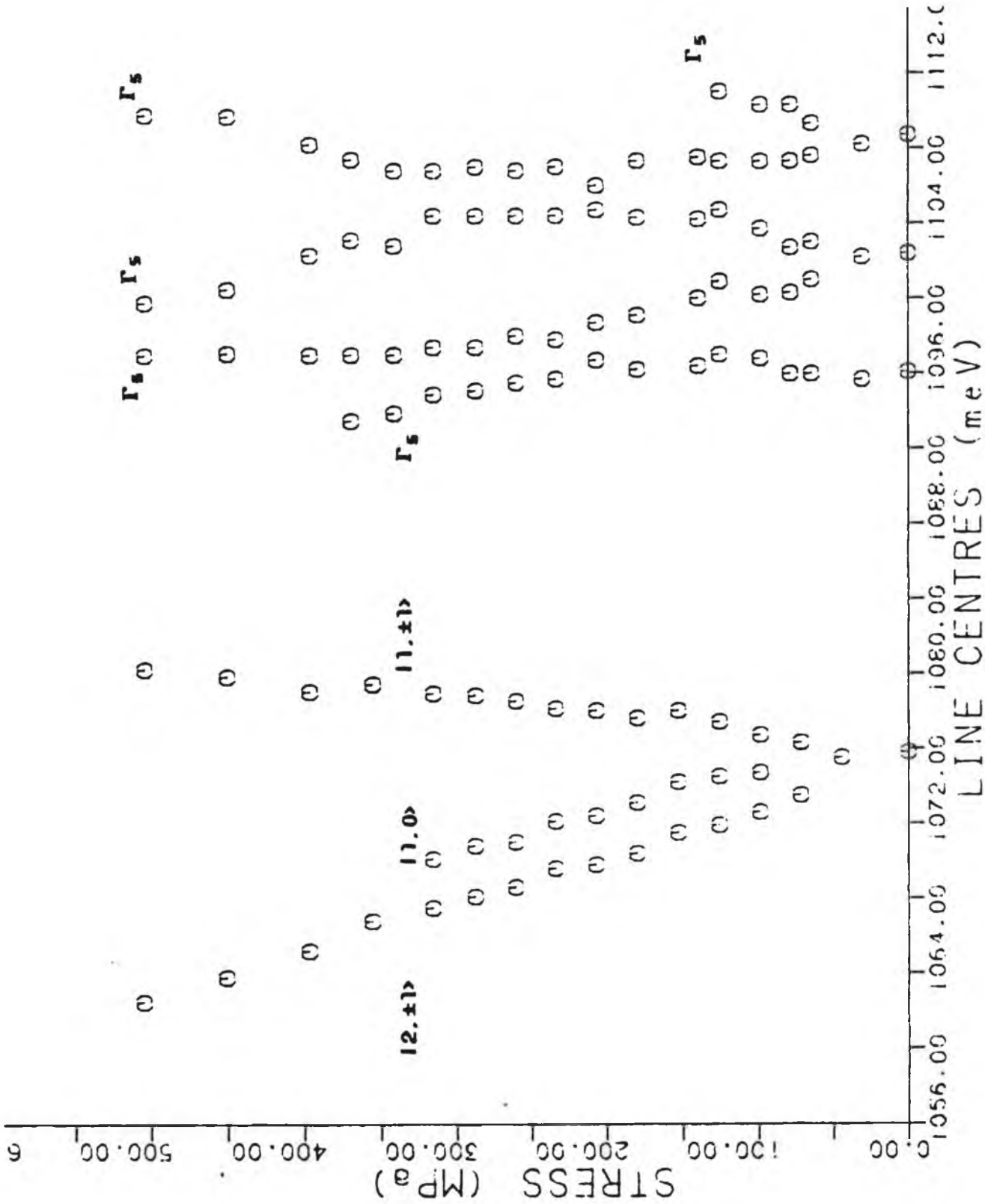

CHAPTER 5

ANALYSIS

5.1 Introduction

The stress results will be analysed to check if they are compatible with the acceptor-like model of the IBE. For such an exciton, as will be explained in section 5.2, the stress splittings originate from the hole states which in turn are derived from the valence band maximum. Three separate aspects of the results are considered; (i) the number of stress split components and their separation, (ii) the values of the deformation potentials deduced from the splitting patterns and (iii) the stress at which the uppermost excited state of the exciton dissociates. These three factors are analysed to establish whether they are as would be expected for an accecptor-like IBE. Before dealing with the results themselves a brief summary of the technique of uniaxial stress analysis is given with particular reference to the valence band maximum in silicon.

5.2 Uniaxial Stress Analysis

The use of external perturbations to characterize the energy levels of a system is a common technique in spectroscopy. Applying a compressive force homogeneously along a crystal axis shifts and, by lowering the crystal symmetry, splits the energy band extrema and, as a result, shallow impurity states also. This procedure is called piezospectroscopy and much of the early work was done by Kaplyanskii (1964). Point defects in a crystal can usually be taken to have the full symmetry group of the host lattice, Td for Si. Non-point defects are often referred to as anisotropic centres as they possess an axis. There are five classes of such defects in the Si lattice, each with a different symmetry group, a subgroup of Td. The axis of an anisotropic centre cannot be randomly oriented in the host crystal but must be directed along an axis of the crystal of the same or higher order. However, the lattice will possess several equivalent such axes so that there is more than one possible orientation for each type of axial defect. This is called orientational degeneracy. The lower the symmetry of an anisotropic centre the greater the multiplicity of its orientational degeneracy as the greater the number of crystal axes along which it can be directed. Compressing a crystal distorts it and changes the energies of all states. The same states of axial centres which are oriented differently with respect to the axis of stress will be shifted by different amounts and therefore

split. Thus uniaxial stress lifts orientational degeneracy. The magnitude of the shifts of each defect will depend on the nature of the defect and on the angle between the stress direction and the axis of the centre. For example, a centre whose axis of symmetry lies along a <100> direction, such as the Be pair, can have three possible different orientations, along <100>, <010> or <001>. Table 1 gives the angles between the pair axis and the stress direction for stress applied parallel to each of a <111>, <100> and <110> direction and the number of components into which each transition at a stressed centre would be expected to split.

Table 1: Lifting of orientational degeneracy for a centre with <100> axis due to different angles between possible centre axes and stress directions.

	<100>	<010>	<001>	no. of components
<100>	0	90	90	2
<111>	45	45	45	1
<110>	45	45	90	2

These are the splittings expected from the lifting of orientational degeneracy only and take no account of the electronic degeneracy which may also be present. As described earlier the maximum possible degeneracy of the electronic levels of a defect are fixed by the number and dimensionality of the irreducible representations of its point group. It follows that a defect of low symmetry will have little or no

removable electronic degeneracy but will have a high degree of orientational degeneracy. The reverse is true of a centre of high symmetry. In fact a centre with symmetry group Td will have no orientational degeneracy but the maximum possible electronic degeneracy.

Stressing the crystal lowers its symmetry and consequently lifts electronic degeneracy. The stress field produced in a homogenous material by a uniaxial compressive force can be resolved into a hydrostatic pressure and a uniaxial shear described by a stress tensor. The hydrostatic pressure produces a uniform shift in all energy levels while the shear shifts states of different representations by different amounts. If the symmetry of a centre is known then for a given stress direction one can calculate what the new smaller group will be. Then using character tables it is possible to work out how the irreducible representations of the original group will reduce under the new symmetry and therefore the number of stress split components expected. More usually one works back from the number of components to the centre symmetry. Obviously some states,such as Kramers doublets, have no removable degeneracy. Thus for an IBE, where the state of the most tightly held particle is always a Kramers doublet, the stress splittings always originate from the loosely held particle. For an acceptor-like IBE the relevant particle is the hole and therefore it is the splittings of the valence band maximum that are of interest here.

The number of the stress split components is therefore determinable purely from group theory but to calculate the size of the splittings perturbation theory is needed. The shifts are taken to be linearly dependant on the strain in the crystal. The $P_{1/2}$ valence band is doubly degenerate and therefore cannot be split. The lower energy $P_{3/2}$ band maximum, which is a Γ_8 state, is four fold degenerate and Chandrasekdar et al (1973) have shown that it splits into two doubly degenerate levels the separation (Δ) of which depends on the stress direction and is given by

$$\Delta_{100} = 2b(S_{11}-S_{12})T \qquad (5.1)$$

$$\Delta_{111} = d/\sqrt{3}\, S_{44}T \qquad (5.2)$$

$$\Delta^2_{110} = \Delta^2_{111} - 4/3(\Delta^2_{111}-\Delta^2_{100}) \qquad (5.3)$$

Here d and b are the deformation potential constants of the valence band for stress along $\langle 111 \rangle$ and $\langle 100 \rangle$ directions respectively. S_{11}, S_{12} and S_{44} are the elastic compliance constants and T is the stress.

As the stress is increased the stress split components of two different lines may approach one another. If the two components have the same irreducible representation they will interact and mix via the strain potential, if not they will just cross.

5.3 Stress induced splitting patterns

The results will be discussed assuming that the IBE is acceptor-like to test the validity of the model.

The most obvious feature of the results presented in chapter 4 is that the splitting patterns are the same for all stress directions. This means that there is no lifting of orientational degeneracy which in turn implies that the symmetry of the axial Be pair is tetrahedral. This apparent contradiction may be explained by comparing the splittings introduced by the axial strain in the 2 K photoluminescence spectra, roughly 2.5 meV, and the line widths of the 85 K absorption spectra , 4 meV approximately. As the latter are larger any axial effects present will not be observable at 85 K. Thus in considering the splittings of the hole states, given the large orbit radius of the hole around the Be pair, the centre may be regarded as having tetrahedral symmetry. Therefore the possible representations of hole states in the unstressed crystal are those given earlier for the top of the valence band, i.e. Γ_6, Γ_7 and Γ_8 . The new symmetry groups which apply for stress along each of the three different directions and the corresponding representations into which these states reduce are given in table 2.

Table 2: Effect of uniaxial stress, along specified axes, on the symmetry and irreducible representations of acceptor states in silicon.

T_d	⟨111⟩ C_{3v}	⟨100⟩ D_{2d}	⟨110⟩ C_{2v}
Γ_6	Γ_4	Γ_6	Γ_5
Γ_7	Γ_4	Γ_7	Γ_5
Γ_8	$\Gamma_4, \Gamma_5+\Gamma_6$	Γ_6, Γ_7	Γ_5, Γ_5

LINE 1: In an acceptor-like IBE the electron, being the more tightly held particle, is in a Γ_1 state. In the ground state of the exciton, which corresponds to line 1 of our spectra, the hole is in its lowest energy Γ_8 state. As mentioned earlier, in section 1.4, the appropriate description of the exciton ground state, in which the electron hole exchange is significant is that which gives its angular momentum quantum numbers. In the presence of an axial strain the ground state splits into five sublevels from three of which, the $|2,\pm1\rangle$, $|1,\pm1\rangle$ and $|1,0\rangle$ states, transitions occur. Transitions from the $|2,\pm1\rangle$ state are partially allowed only by virtue of mixing with the $|1,\pm1\rangle$ state and thus are not observed in the unstressed 85 K absorption spectrum . However under stress the transition becomes stronger. The other two transitions are too close to be resolved at 85 K but under stress their separation increases giving the three stress split components with stress dependent intensities seen for line 1. The separations under

high stress of these components are in reasonable agreement with the calculations of Mathieu et al (1980) who give the energy of the different $|J,M_j\rangle$ exciton states under high stress as :

$$E(|1,\pm1\rangle) = 3\gamma/8 + \epsilon \qquad (5.4)$$

$$E(|1,0\rangle) = 5\gamma/8 - \epsilon - \epsilon'^2/(\Delta o + \epsilon) \qquad (5.5)$$

$$E(|2,\pm1\rangle) = -1\gamma/8 - \epsilon - \epsilon'^2/(\Delta o + \epsilon) \qquad (5.6)$$

where γ is the exchange splitting, 2ϵ is the stress splitting of the valence band maximum, Δo is the spin-orbit splitting of the valence band and the second order term in ϵ' gives the energy shift due to the stress-induced coupling between the $M_j=1/2$ components of the $P_{3/2}$ and $P_{1/2}$ valence band maxima. At high stresses $\epsilon>>\gamma$ and $\epsilon>>\epsilon'$. Thus the separation of the $|1,\pm1\rangle$ and $|1,0\rangle$ components is roughly 2ϵ. This is just the Γ_8 valence band splitting and, as will be shown later, is the same as the separation of the components of lines 3 and 4. Equations 5.5 and 5.6 show that the separation of the $|1,0\rangle$ and $|2,\pm1\rangle$ components should be stress independent and equal to $3/4\gamma$, i.e. 75% of the J-J splitting which, for the Si:Be IBE, is approximately 2 meV (Kiloran et al (1982)). The observed separation is roughly 2 meV and is stress independent, see figures 4.2-4.4. Thus the agreement between our data and the

theory is quite good.

LINE 2: Whereas the exciton ground state is best desscribed in the $|J,M_j\rangle$ notation, the other exciton states are best described in terms the irreducible representations of the hole and electron states. Line 2 does not split under stress and, from table 2, this implies that the hole state is either Γ_6 or Γ_7. There is considerable theoretical support for the existence of a low lying Γ_7 state for effective mass acceptors in silicon (Lipari and Baldereschi (1978)). Labrie et al (1984) argue that the separation of lines 1 and 2 favours a Γ_7 identity for this hole state. Our data is therefore consistent with this identification of the first excited state of the exciton.

LINES 3 and 4: Both lines 3 and 4 split into two components for all stress directions and thus the unstressed hole state of each must be Γ_8. Assuming that Γ_7 is the correct representation for line 2, it is possible, using table 2, to deduce the representations of the components of line 3 from the interaction between line 2 and the lower energy component of line 3 . It follows that the representations of the lower energy component under stress along $\langle 100 \rangle$, $\langle 111 \rangle$ and $\langle 110 \rangle$ are Γ_7, Γ_4 and Γ_5, respectively, while the corresponding representations of the higher energy component are Γ_6, $\Gamma_{5,6}$ and Γ_5. There is evidence, though not as clear, of interaction between the higher energy component of line 3

and the lower energy component of line 4. Accordingly the low and high energy components of line 4 are labelled Γ_6, $\Gamma_{5,6}$ and Γ_5 and Γ_7, Γ_4 and Γ_5 for stress along ⟨100⟩, ⟨111⟩ and ⟨110⟩ respectively. A similar reversal of the ordering of stress split hole states has been observed for acceptors in silicon (Chandrasekahr et al (1973)). Thus the stress splittings are consistent with the acceptor like model.

5.4 Deformation Potentials

Compressing a crystal produces strain in it. The elastic compliance constants of a material relate the strain in a crystal to the different stresses, both compressive and shear, which are generated when the crystal is subjected to a compressive force. For uniaxial forces along the ⟨100⟩, ⟨110⟩ and ⟨111⟩ axes only three of the thirty six elastic compliances are needed to calculate the strain produced. Strain in a crystal modifies its electric field and thereby changes the energies of its states. The deformation potentials relate the resultant energy shifts to the strain that produces them. Two independent deformation potentials, b and d, are needed for each energy level.

It is possible to estimate the values of the deformation potentials b and d for the valence band maximum from the separations of the stress split components of lines 3 and 4,

and from that of the two higher energy components of line 1, using equations 5.1-5.3 and the published (Laude et al (1971)) values of the elastic compliances of silicon:

S_{11}= 0.863, S_{12}= -0.213, S_{44}= 1.249 x10^{-11} Pa^{-1}.

Our results (sample calculations are included in appendix 3) are presented in table 3 where they are compared with the free exciton values obtained by Laude et al (1971). Our values for d are in approximate agreement with those for the free exciton while our b values are roughly 50% smaller. This is in marked contrast to the donor-like IBE in GaP:Bi (Onton and Morgan (1970)) where an order of magnitude reduction is found in the value of b. This futher supports the acceptor like classification of the Be pair IBE.

Table 3: Deformation potentials b and d for Γ_8 holes in the Si:Be bound exciton.

	Line 1	Line 3	Line 4	Free Exciton(a)
b(eV)	1.35	1.3	1.1	2.10 ± 0.10
d(eV)	3.5	4.0	3.9	4.85 ± 0.15

The values estimated for b and d are accurate to 10%.
(a) Laude et al (1971).

5.5 Dissociation of the exciton

Both the unstressed hole state in line 4 and the top of the $P_{3/2}$ valence band are Γ_8 states. It follows that under stress they will both split into two components the separation of which is given by equations 5.1-5.3. At some stress, see figure 5.1, the high energy component of line 4 will therefore coincide with the low energy component of the valence band maximum. At this stress the line should disappear as the exciton will dissociate, the hole being free in the valence band. As the hydrostatic shift of both states is the same the rate of approach (R) of the high energy component of line 4 and the lower energy top of the valence band state is the sum of the shift rate to higher energy of the former and the shift rate to lower energy of the latter. For stress along <111> this is given by:

$$R = d/\sqrt{3}\, S_{44} T \qquad (5.7)$$

Similar expressions can be derived for the other two stress directions. When this equals the initial unstressed separation of line 4 and the valence band maximum then the component should vanish. According to Labrie et al (1984) the IBE is acceptor-like with a hole binding energy of 43 meV. From our data the difference in hole energy between the exciton ground state (line 1) and the third excited state (line 4) is 33.2 meV (1109.5-1075.7 meV) and therefore the

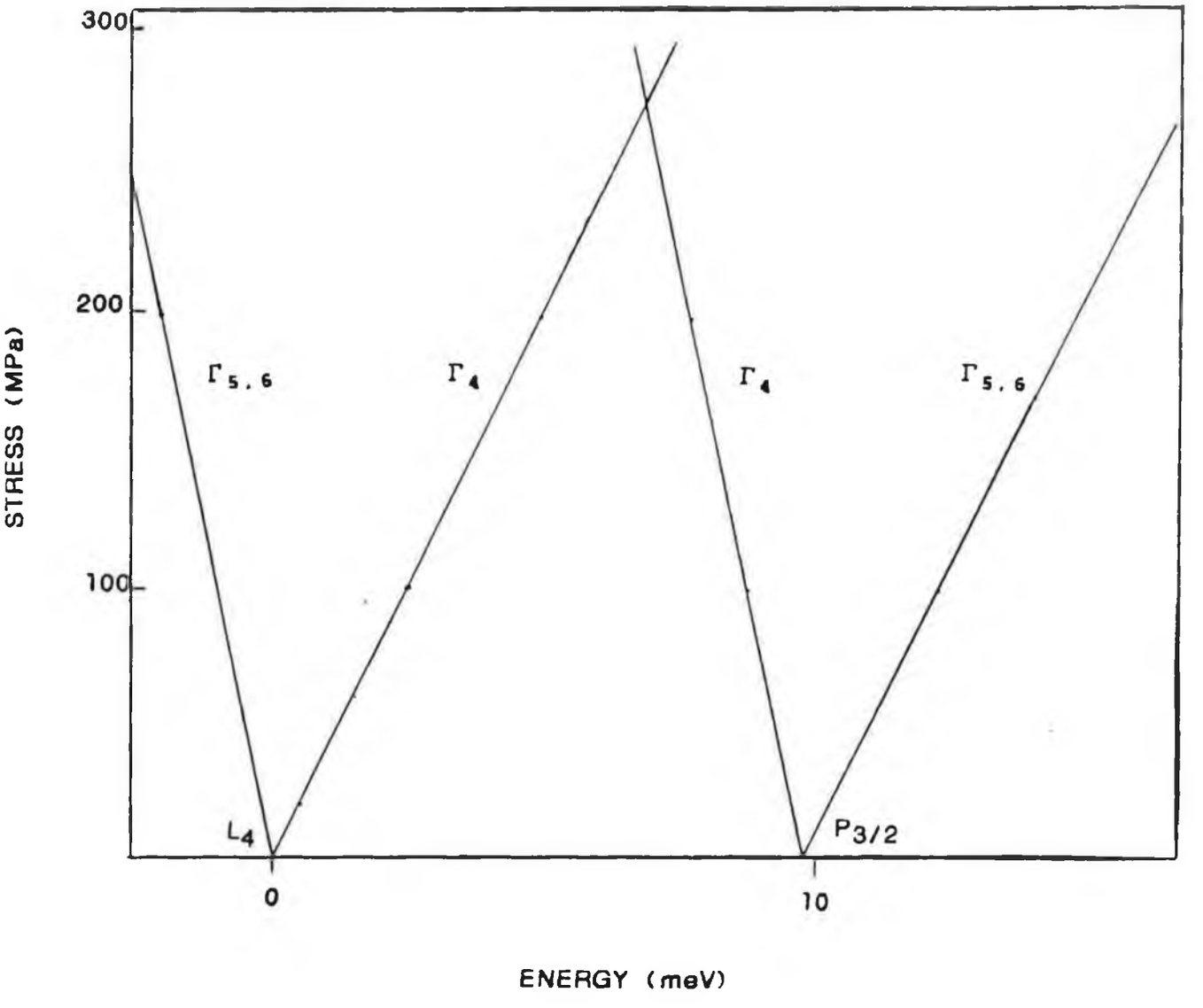

Fig. 5.1 : *Dissocciation of the exciton*
The splittings and shifts of the two Γ_8 states, the hole of the third excited exciton state (L_4) and the top of the $P_{3/2}$ valence band are shown for stress along <111>. These were calculated using the equations of Chandrasekaer et al (1973). It is clear that at a stress of 280 MPa the upper Γ_4 hole state coincides with the lower Γ_4 valence band edge. The exciton will therefore dissociate at this stress as the hole becomes free in valence band.

binding energy of the hole in line 4 is 9.8 meV. Thus for a stress of approximately 280 MPa along <111> the high energy component of line 4 should vanish. In fact our last recorded position for it is at 190 MPa. This component is very weak at all stresses and very difficult to extract from the noise and may actually persist beyond this stress value. However the fact that it is definitely gone at 280 MPa may be taken as supportive of the acceptor assignment.

5.6 Conclusion

In this study the technique of uniaxial stress analysis was used to examine in detail a defect in silicon. The above discussion shows that the stress data for the Si:Be absorption spectra can be explained very successfully in terms of an acceptor like model for the IBE. Together with the evidence of Labrie et al (1984) cited in chapter 2 this confirms the acceptor like assignment of the centre, demonstrating the usefulness of the technique.

CHAPTER 6

Conclusion

This study examined the near infra-red absorption spectrum of the beryllium pair related exciton in silicon under stress. The centre had already been identified from its low temperature luminescence, including Zeeman studies, as being bound to an axial isoelectronic centre, with a ⟨100⟩ axis, which is as would be expected for an exciton trapped at a pair of Be atoms in silicon. However there was some confusion as to whether the IBE was acceptor or donor-like and it was hoped that by investigating the stressed absorption spectra the problem would be resolved. To that end an experimental system was developed to record the NIR absorption spectra of stressed samples at liquid nitrogen temperatures and to extract the exciton features from the strong background water vapour absorption present in the wavelength region of interest. The results obtained are consistent with the acceptor-like model of the exciton and in particular support the assignent of a Γ_7 state to the first excited state of the exciton. The classification of the centre is therefore complete.

APPENDIX 1

Printed circuit board layout for spike removal unit

APPENDIX 1

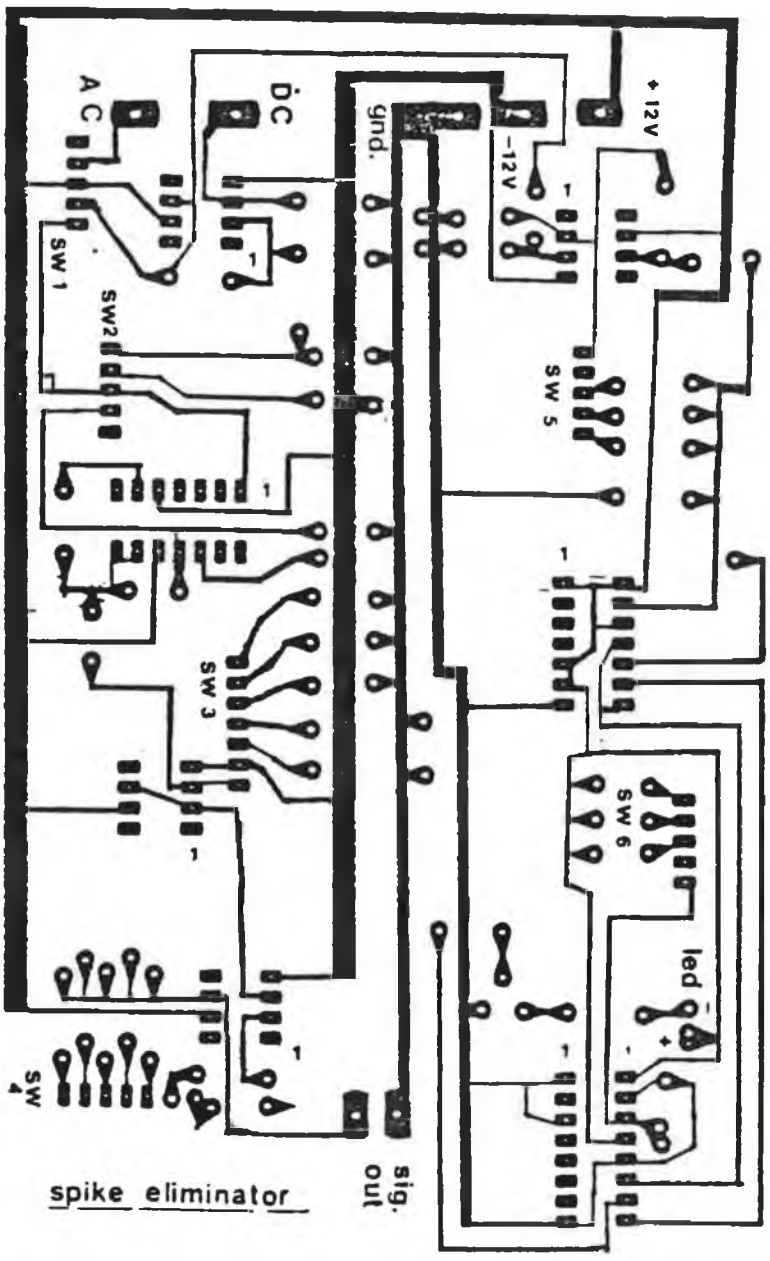

P. C. B. layout of spike removal unit.

APPENDIX 2

Program used to control monochromator and to record and process spectra

```
  5 REM INITIALISATION
 10 DIM S%(300),B%(300),COEFF(302)
 14 INPUT"STARTING WAVELENGHT" START
 16 INPUT"INCREMENT" INC
 20 A=&FCF0
 30 ?(A+11)=&C0
 40 ?(A+2)=&70
 50 ?(A+4)=6:?(A+5)=0
 55 D=&FCC0
 60 ?(D+3)=128
 80 MODE4
100 REM MENU
102 CLS
105 PRINTTAB(10,5)"MENU"
110 PRINT:PRINT" 1. MENU"
115 PRINT" 2. BASELINE"
120 PRINT" 3. SIGNAL"
125 PRINT" 4. BACKGROUND"
130 PRINT" 5. REMAINDER"
135 PRINT" 6. MANIPULATE"
150 PRINT" 8. CHART"
160 PRINT"10. EXIT"
165 PRINT:PRINT
170 INPUT"INPUT NO. OF OPTION REQUIRED " CHOICE
175 IF CHOICE<11 AND CHOICE>0 THEN GOTO CHOICE*100
180 GOTO 100
200 REM BASELINE
202 CLS
205 PRINT"SHUT SLIT TO MONITOR DETECTOR D.C."
210 PRINT"HIT ANY KEY WHEN READY"
215 BASE=0
220 K=GET:C=0
225 FOR I=1 TO 10
230 PROCread:PRINT INF
240 C=C+INF
250 NEXT I
260 BASE =C DIV 10
272 PRINT "AVERAGE D.C.="BASE
290 K=GET
295 GOTO 100
300 REM SIGNAL
310 GOSUB 2000
320 CLS
330 FOR I=1 TO 300
332 AVE=0
335 FOR J=1 TO 36
340 PROCread
344 AVE=AVE+INF
348 NEXTJ
350 S%(I)=AVE DIV 36
360 PLOT 69,4*I,S%(I)/2.4
365 PROCtrig
368 FOR K=1 TO 400:NEXT K
370 NEXT I
390 K=GET
395 GOTO 100
400 REM BACKGROUND
410 GOSUB 2000
420 CLS
430 FOR I=1 TO 300
432 AVE=0
435 FOR J=1 TO 36
440 PROCread
444 AVE=AVE+INF
448 NEXT J
```

```
450 B%(I)=AVE DIV 26
460 PLOT 69,4*I,B%(I)/2.4
465 FOR K=1 TO 400:NEXT K
470 PROCtrig
480 NEXT I
490 K=GET
495 GOTO 100
500 REM REMAINDER=COEFF
505 CLS
508 PRINT
510 INPUT"HAVE YOU DONE A BACKGROUND"Q
520 IF Q=0 GOTO 100
522 CLS
525 MAX=0:MIN=10000
530 FOR I=1 TO 300
540 COEFF(I)=(B%(1)-S%(I))/B%(I)
545 IF COEFF(I)>MAX THEN MAX=COEFF(I)
550 IF COEFF(I)<MIN THEN MIN=COEFF(I)
555 NEXT I
560 CLS:SCALE=1023/MAX
565 FOR I=2 TO 298
567 PLOT 69,4*I,SCALE*COEFF(I)
569 Z=COEFF(I+1)+COEFF(I-1)
571 Y=COEFF(I+2)+COEFF(I-2)
572 COEFF(I)=.4*COEFF(I)+.2*Z+.1*Y
575 NEXT I
577 K=GET:CLS
579 PRINT
580 INPUT"DO YOU WANT TO MANIPULATE"Q
585 IF Q=1 GOTO 600 ELSE GOTO 100
600 REM MANIPULATE
602 INPUT"INPUT SUBTRACTION FRACTON "SF
605 CLS
608 VDU 24,0;140;1279;1023;
610 VDU 28,0,31,36,28
615 SLOPE =(COEFF(256)-COEFF(1))/255
620 MAX=MAX-SF*MIN
625 SCALE=1000/MAX
630 FOR I=1 TO 300
635 ADJ=SLOPE*I+SF*MIN
645 COEFF(I)=COEFF(I)-ADJ
655 PLOT 69,4*I,COEFF(I)*SCALE
670 NEXT I
700 REM CURSOR
710 MOVE 0,0
720 J=0
730 IF GET=70 THEN PROCforward
735 IF GET=66 THEN PROCback
740 IF GET=76 THEN PROCwl
745 IF GET=69 GOTO 750
748 GOTO 730
750 VDU 26:GOTO 100
800 REM CHART
802 T(D+2)=128
805 PRINT"HIT ANY KEY WHEN READY"
807 K=GET
810 MULT=4000/MAX
820 FOR I=1 TO 300
830 X=COEFF(I)*MULT
840 PROCwrite(X)
850 FOR J=1 TO 50 :NEXT J
870 NEXT I
875 TD=0
880 GOTO 100
1000 END
1100 DEF PROCread
```

```
1105 REM READS IN DETECTOR OUTPUT
1110 ?A=16
1120 ?(A+12)=12
1130 ?(A+12)=14
1140 INP=(?(A+1))*16+ (?A) MOD 16
1150 INP=2048-INP-BASE
1190 ENDPROC
1200 DEF PROCwrite(X)
1210 REM SENDS TO CHART
1230 ?D=X*16:?(D+1)=X MOD 16
1250 FOR J=1 TO 400:NEXT J
1290 ENDPROC
1300 DEF PROCfoward
1305 REM MOVES CURSOR FOWARD IF F HIT
1310 PLOT 6,4*J,0
1320 J=J+1
1330 MOVE 4*J,0
1340 PLOT 5,4*J,COEFF(J)*SCALE-5
1350 GOTO 730
1400 DEF PROCback
1405 REM MOVES CURSOR BACK IF B HIT
1410 PLOT 6,4*J,0
1420 J=J-1
1430 MOVE 4*J,0
1440 PLOT 5,4*J,COEFF(J)*SCALE-5
1450 GOTO 730
1500 DEF PROCwl
1505 REM PRINT WAVELENGHT IF L HIT
1510 WL=J*INC +START
1520 U=J DIV 9
1530 PRINT;TAB(U) WL
1550 GOTO 730
1600 DEF PROCtrig
1605 REM SENDS TRIGGER PULSE TO SPEX
1610 ?(A+12)=&E0
1620 ?(A+12)=&C0
1630 ?(A+12)=&E0
1680 ENDPROC
2000 REM ADJUSTMENT
2001 CLS
2005 PRINTTAB(0,4)"ADJUST FOR MAX SIGNAL"
2010 PRINTTAB(0,5)"HIT R WHEN READY"
2015 PRINTTAB(0,6)"HIT E TO EXIT "
2020 REPEAT
2030 PROCread
2040 PRINTTAB(0,1) INP
2050 IF INKEY(1)=-9 GOTO 100
2060 UNTIL INKEY(1)=-82
2090 RETURN
```

APPENDIX 3

Estimation of the deformation potentials b and d from the stressed splitting patterns.

A Γ_8 hole state in silicon splits under stress into two components whose separation for pressure applied along different crystal axes is given by equations 5.1-5.3 . Three of the exciton states we observed in Si:Be, those involved in lines 1, 3 and 4, have Γ_8 hole states. Therefore from the separation of the stress split components of these lines the deformation potentials can be determined. In the case of line 1 three components are observed due to exchange interaction, however the separation of the two higher energy components is the Γ_8 splitting. These components do not undergo interactions with other stress split components and thus their separation is a linear function of stress. From equation 5.1 the slope of their separtion (Δ) plotted against stress along $\langle 100 \rangle$ should give the value of b while the slope of their separation against stress along $\langle 111 \rangle$ yields d, the values of the elastic compliances being known.

A linear least squares fit of the separation (Δ_{100}) of the two higher energy components of line 1 under $\langle 100 \rangle$ stress has a slope of 2.898×10^{-11} eV/Pa which gives a value of 1.34 eV for b. A fit of the separation (Δ_{111}) against

stress along ⟨111⟩ has a slope of 2.5 x 10^{-11} eV/Pa giving d a value of 3.5 eV.

The stress split components of lines 3 and 4 interact with each other and line 2 so that a linear fit is not possible. Instead we evaluate the deformation potentials from the separation of the components of each line for a pressure of 95 MPa. For line 3; Δ_{100} at 95 MPa is 2.70 meV giving b = 1.3 eV. Δ_{111} is 2.61 meV giving d = 3.8 eV.

REFERENCES

Chandrasekhar H R, Fisher P, Ramdas A and Rodriguez S 1973 Phys. Rev. B 8 3836-50

Collins A T and Jeffries T 1982 J. Phys. E. Sci. Istrum. 15 712-6

Crouch R K, Robertson J B and Gilmer T E Jr 1972 Phys. Rev. B5 3111-9

Dean P J and Herbert D C 1979 "Excitons; Springer Topics in Current Physics" vol 14, ed. K Cho (Berlin: Springer)

Elliot J P and Dawber P G "Symmetry in Physics" Macmillan London (1979)

Fisher P and Ramdas A K "Physics of the Solid State" ed. S Balakrisna Academic New York (1969)

Heine V "Group Theory in Quantum Mechanics" McGraw Hill New York (1964)

Henry M O, Lightowlers E C, Killoran N, Dunstan D J and Cavenett B C 1981 J. Phys. C: Solid State Phys. 14 L255-61

Henry M O Pers. Comm.

Hopfield J J, Thomas D G and Lynch R T 1966 Phys. Rev. Lett 17 312-5

Kaplyanskii G 1964 Optics Spectra. 16 557

Kiloran N, Dunstan D J, Henry M O, Lightowlers E C and Cavenett B C 1982 J. Phys. C.:Solid State Phys. 15 6067

Kirczenow G 1977 Solid State Commun. 21 713-7

Kohn W and Luttinger J M 1955 Phys. Rev. 98 915-25

Labrie D, Timusk T and Thewalt M L W 1984 Phys. Rev. Lett 52 81-84

Laude L D, Pollak F H and Cardona M 1971 Phys. Rev. B 3 2623-36

Lipari N and Baldereschi A 1978 Solid State Commun 25 665

Maeda K 1965 J. Phys. Chem. Solids 26 595-7

Mathieu H, Bayo L, Camassel J and Merle P 1980
Phys. Rev. B 22 4834-48

Morgan J van W and Morgan T N 1970 Phys. Rev. B 1 739-49

Onton A and Morgan T N 1970 Phys. Rev. B 1 2592-2605

Ramdas A K and Rodrigues S 1981 Rep. Prog. Phys. 44 1297

Shaklee K L and Nahory R E 1970 Phys. Rev. Lett. 24 942

Thewalt M L, Watkins S P, Ziemelis U, Lightowlers E C and
Henry M O 1982 Solid State Commun. 44 573-8

Tinkham M "Group Theory in Quantum Mechanics"
McGraw Hill New York (1964)

Watkins S P, Thewalt M L W and Steiner T 1984
Phys. Rev. B 29 5727-38

Acknowledgements

I would like to thank my supervisor, Dr. Martin Henry, for his constant advice, enthusiasm and patience throughout the preparation of this thesis. I am indebted to Dr. Frank Mulligan for his expert advice on many computing problems. I am also grateful to Alan Hughes for his assistence in the design and construction of the electronics and to all the technicans of the School of Physical Sciences.

I would like to acknowledge the support of the Research and Postgraduate Studies committee of NIHE Dublin.